ETH
Eidgenössische Technische Hochschule Zürich
Swiss Federal Institute of Technology Zurich

Institute for
Dynamic Systems and Control
IDSC
Institut für Dynamische Systeme
und Regelungstechnik

Antonia Mosberger

Advanced Driver Assistance Systems on a Go-Kart

Bachelor Thesis

Institute for Dynamic Systems and Control
Swiss Federal Institute of Technology (ETH) Zurich

Supervision

Prof. Dr. Emilio Frazzoli
Jan Philipp Hakenberg

July 2019

IDSC-proj-bt-am

Abstract

Advanced Driver Assistance Systems (ADAS) have the purpose to increase the road traffic safety by reducing driver errors, to make the driving experience more comfortable and to enhance the efficiency of the vehicles.
In the context of my bachelor thesis, three different ADAS are implemented on a go-kart provided by the IDSC group.

- The electric power steering supports the driver in his task to steer the vehicle by applying an assistant torque. Additionally, the aligning torque, which restores the steering wheel towards the initial position, is compensated.
- The lane keeping assistant prevents the driver from leaving the lane by indicating a safe steering direction to the driver. So, the go-kart will be led back to a safe position on the lane.
- The anti-lock braking system increases the vehicle steerability during a full braking and shortens the braking distance.

The features were evaluated by testing them on the said hardware. For all three ADAS, the main objectives set in advance were achieved. Therefore, the thesis contributes to the vision of the IDSC go-kart project: carry out research on the edge cases and extreme situations of autonomous driving.

Keywords: Advanced Driver Assistance Systems, ADAS, Autonomous driving, Electric Power Steering, Anti-lock Braking, Lane Keeping Assistant

Acknowledgement

I am grateful to everyone who supported me during this bachelor thesis.

Firstly, I want to thank my supervisor Jan Philipp Hakenberg. He supported me by answering my questions and providing thought-out advise. After our meetings, I had clear goals for the further progress and felt motivated. I really appreciate his supervision approach that encouraged my personal progress and learning.

I want to thank the Frazzoli group, the IDSC and ETH Zurich for providing the infrastructure for the go-kart project. Having the possibility for students to work within the highly interesting field of autonomous driving is an evidence for the high quality of the education at ETH.

To work with everyone involved with the go-kart was highly motivating. Not only did everyone support the projects of the others with ideas and advice. Due to meeting each other up to three times a week, it was possible to develop personal friendships.

Writing a bachelor thesis has challenged me, but hence taught me a lot. This experience is valuable to me and will be an incentive for my future studies.

Zurich, August 2019

Antonia Mosberger

Nomenclature

Acronyms and Abbreviations

ADAS	Advanced Driver Assistance Systems
ABS	Antilock Brake System
DAS	Driver Assistance Systems
ESC	Electronic Stability Control
EPS	Electric Power Steering
ECU	Electronic Control Unit
ETH	Swiss Federal Institute of Technology Zurich
GNSS	Global Navigation Satellite System
IDSC	Institute for Dynamic Systems and Control
IIR filter	Infinite Impulse Response filter
IMU	Inertial Measurement Unit
Lidar	Light detection and ranging
MPC	Model Predictive Control
PID	Proportional-Integral-Derivative (Controller)
SCE	Steering Column Encoder
SCT	Steering Column Torque
TCS	Traction Control System

Contents

Chapter 1

Introduction

1.1 Objectives of ADAS

Participating in the road traffic, be it as a pedestrian, as a bicycle rider or as a car driver, always means putting your life at risk. In 2017, 25'300 people lost their life on European roads and 135'000 get seriously injured [1]. By analyzing road crashes, it was found that a driver error is in up to 95% of the cases at least partly the cause for an accident (compared to 34% environmental factors and 13% vehicle factors), whereby the driver error was defined as "errors of recognition, errors of decision, and errors of performance" [2, 3, 4].

In order to make road traffic safer by reducing the share of human errors in accident causes, it stands to reason that the best measure is to support the driver in his highly complicated task. Advanced Driver Assistance Systems (ADAS) do this by preparing the environment information perceived by the sensors for the driver (e.g. Blind Spot Monitor), by alerting the driver when entering potentially dangerous situations (e.g. Driver Drowsiness Detection), by imposing restrictions on the driving behaviour and in this way preventing the driver of getting into dangerous situations (e.g. Lane Keeping Assistant), and by taking over the control of the vehicle when the driver already is in a dangerous situation (e.g. Autonomous Emergency Braking).

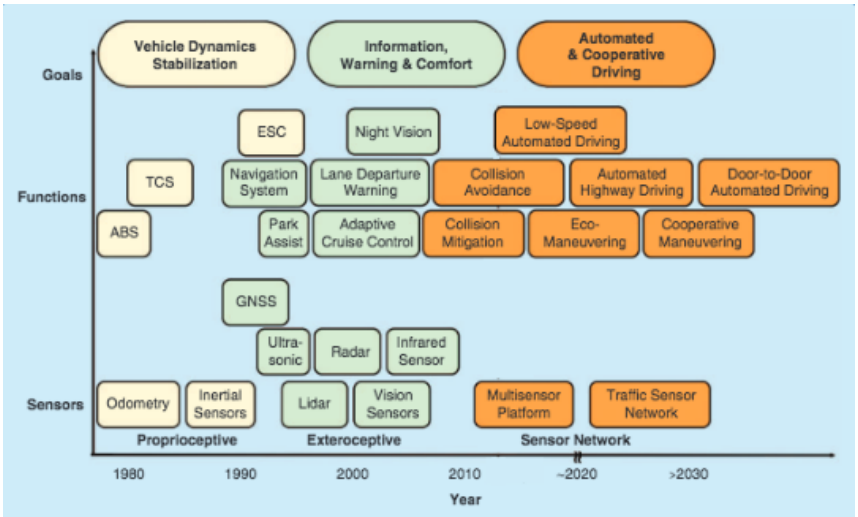

Figure 1.1: Past and potential future evolution towards automated cooperative driving [5].

Summarized, the most important objective of ADAS is improving road safety. Some ADAS such as ABS (Antilock Brake System) or ESC (Electronic Stability Control, an evolution of ABS) are even made a legal requirement by the European Union for new cars [6], due to their big impact on accident prevention [7].

As it can be seen in figure 1.1, the development of ADAS has started 40 years ago with the first ABS (Bosch has been producing ABS in serial production since 1978 [8]). The early generation of DAS (Driver Assistance Systems) was based on proprioceptive sensors which measured only the internal states of the vehicle, and enabled a better control over the vehicle's dynamics. Around 1990, a second generation of advanced DAS, so called ADAS, was introduced, which focused on providing information and warnings to the driver and on enhancing the driving experience. These new functions rely on exteroceptive sensors, which collect information about the environment around the vehicle [5].
In the past 20 years, a lot of effort was put into the research towards autonomous driving. In this ongoing process, ADAS play a key role. Firstly, autonomous applications are often derivatives from ADAS (for example, the Lane Keeping Assistant emerged directly from the Lane Departure Warning System). Secondly, ADAS are the forerunner to gain acceptance for fully autonomous vehicles.

Figure 1.2: Photography of the testing area [9].

1.2 Motivation

The go-kart project has been an ongoing project since December 2017 at the IDSC (Institute for Dynamic Systems and Control) at ETHZ (Swiss Federal Institute of Technology Zurich) of Prof. Frazzoli. The research goal of the project is to investigate the behaviour of the go-kart in extreme dynamic situations. As a side effect, the go-kart is a great learning platform for students who are interested in autonomous driving.
In the scope of this thesis, three different ADAS are implemented. Not all ADAS that are meaningful on a car are meaningful on a go-kart (e.g. a blind spot monitor). So the main criteria to select the projects was how useful they are for the go-kart project as a whole. Out of the many ADAS that the automotive industry came up with, the following three were chosen.

Although the go-kart project is about autonomous driving, many of the drives are in manual mode, mostly for testing purposes. The steering system of the go-kart requires a high driver torque which feels uncomfortable for the driver. So, as a first project, an **EPS (Electric Power Steering)** is implemented on the go-kart. An EPS applies a driver assist torque at the steer column, which supports the driver in his task to steer the vehicle.

According to research on accidents, around 65% (exact numbers are varying between the studies) of fatalities in single-vehicle crashes are due to the vehicle leaving the lane, so called run-off-road

crashes [10, 11, 12]. Based on this, the huge potential of **lane keeping assists** was recognized by the automobile industry. Starting with lane departure warning systems, many car companies enhanced this feature into a lane keeping assist which actively helps the driver to stay on the road [13].

For many modules implemented on the go-kart, braking is an essential functionality.
For example, the full braking is needed in the demonstration module "Emergency Brake Maneuver", where the go-kart performs an emergency brake as soon as an object appears in front of it. Another example is the MPC mode, which uses a model predictive control approach to autonomously race a given track as fast as possible (refer to [9]). This challenges the brakes of the go-kart, since they are active most of the time. On the other hand, the braking behaviour has a big impact on the MPC itself: the braking distance and the stability during a braking process set the limits for the planning of the MPC. Therefore, an improvement of the braking process could lead to improvements of the MPC.
Due to the big impact of an improvement of the full braking maneuver on the go-kart project, it was decided to design an **ABS (Anti-lock Braking System)** for the go-kart.

1.3 Structure of the Document

The report of the thesis is structured in the following way: Each ADAS which is implemented in the scope of this thesis has its own subsection in each chapter. So, it is possible to cross read, meaning that one can read first just the documentation for example of the lane keeping assist, and then continue with the next ADAS.

Chapter 2

Problem Formulation

In this chapter, the motivation for each ADAS is outlined in detail. The needed background knowledge of the physical system and of the preconditions is provided. Afterwards, the objectives are derived from the problem description. Quantitative goals are added in order to ensure the measurability of the objectives.

2.1 Testing Platform

The go-kart is equipped with an IMU (Inertial Measurement Unit), a Lidar sensor and an Event Based Camera in order to collect the necessary information about its environment. The brakes are accentuated by a linear motor, and the rear wheels are driven with servo motors. The testing area is in an old hangar in Dubendorf. The objectives stated in this chapter are verified with test drives on that go-kart.

2.2 Electric Power Steering

EPS (Electric Power Steering) has several objectives, depending on the driving mode.

During manual driving, EPS is needed to reduce the steering torque felt by the driver which will eventually improve the whole driving experience. This is achieved by adding a controlled assist torque to the steering column, that helps the driver to rotate the steering wheel. Since the driver isn't obstructed by a large steering torque, he has a better control over the vehicle.

In the autonomous driving mode, not a driver, but a PID controller converts the wanted steering angle into a steering torque. Due to the steering system behaviour described in the next paragraph, the PID controller reached the demanded steering angle inaccurately.

The pivot line (steering column direction) of the wheel contacts the floor in front of the wheel's centerline. These two lines draw up the caster angle (see fig. 2.1). The lateral velocity on the wheel induces a force perpendicular to the wheel. This force in turn induces a so called aligning torque which straightens the steering wheel while driving forward. On one hand, this effect makes it easier to steer the vehicle by reducing it's tendency to wander, especially for high speed driving. On the other hand it is a disadvantage for autonomous steering:
Assumed, the PID controller, implemented in modules such as the MPC and responsible for curve following, tries to reach a given, constant steering angle θ_{given} in order to follow the trajectory (see fig. 2.2). The P-part multiplies the error between θ and θ_{given} with a constant. This results in a constant error-compensating torque which is counteracted by the aligning torque. In this state, the D-part has no influence since θ is not moving anymore. The I-part of the controller will slowly sum up the error and θ_{given}, which is still constant, will be reached over time. But

since most trajectories don't consist of a constant steering angle, but of a succession of angles, the time depending I-part does not adapt fast enough to the new input and therefore the controller accomplishes his task to follow the trajectory inaccurately.

Out of the previous problem description, two goals have been derived:

- When the power steering module is active, the **steering torque applied by the driver has to be reduced** compared to a similar ride without power steering. Unfortunately, it is not possible to have a direct comparison of the same ride with and without power steering. Instead, it is tried to compare as similar drives as possible, and it is made sure to have a large data basis for comparison.

- The power steering should **compensate the aligning torque**, since it is a disturbance for the PID controller. This is measured by the deflection of the steering angle, when no torque is applied by the driver. The elimination of the aligning torque is prioritized over the return-ability of the steering wheel which would improve the steering stability of the vehicle.

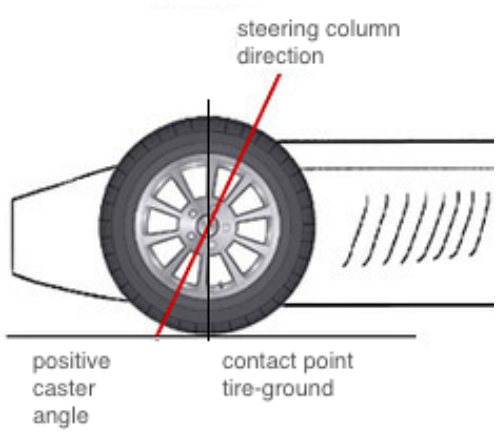

Figure 2.1: Visualization of a positive caster angle [14].

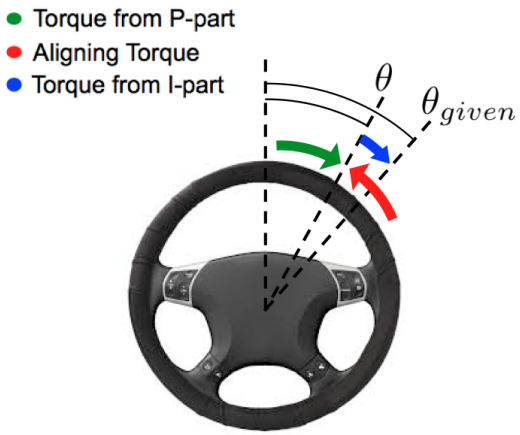

Figure 2.2: Visualization of the PID controller behaviour.

2.3 Lane Keeping Assist

A lane keeping assist provides brief gentle input to the steering wheel to help prevent the driver from unintentionally leaving the lane. The assist just intervenes when it's foreseeable that the driver is going to leave the lane, but is passive during a safe drive. Further, the lane keeping assist can not enforce a maneuver; the driver has always the option to leave the lane if this is his intention.

The following objectives can be formulated for the lane keeping assist implemented on the go-kart.

- If the driver is about to leave the lane by applying a medium driver torque (< 0.8[SCT]), the lane keeping assist will **keep him on the lane**. The maximum distance between the go-kart and the lane boundary is measured for a medium and no applied driver torque.

- If the driver wants to **leave the lane intentionally** by applying a high driver torque (> 0.8[SCT]), the lane keeping assist can not enforce him to stay on the lane.

- The lane keeping assist can lead the vehicle back with **smooth steering movements** and without provoking the steering wheel to oscillate.

2.4 Anti-lock Braking System

In a nutshell, the working principle of an ABS is the following: The ABS controls the force of the brake chocks on the wheel. This leads to varying degrees of blockade of the wheel, which impacts the braking behaviour. The advantages of ABS are outlined in this section.

A rolling wheel always tries to avoid slip. Therefore, the no-slip condition says that the velocity in the contact point between tire and ground always has to be zero (see fig. 2.3). When the driver turns the steering wheel, the steering mechanism turns the wheel, so the rotational velocity is inclined. Since the velocity in the contact point still has to be zero, the translational velocity is also inclined and the vehicle turns (see fig. 2.4).
In a braking process without ABS, the brakes will block the turning of the wheel. In this case, the rotational velocity can not enforce the translational velocity to incline, since the rotational velocity is zero. The vehicle isn't steerable anymore.

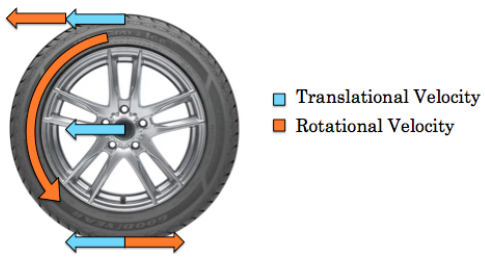

Figure 2.3: The no-slip condition as an illustration. The translational and rotational velocity in the contact point with the ground cancel out.

Figure 2.4: The inclined rotational velocity makes the translational to incline as well, since the no-slip condition has to be fulfilled. So, the vehicle changes its direction.

The ABS is designed to solve this problem. By adjusting the pressure of the brake chock on the tire, the rotational velocity is not always zero during the braking process, but is is sometimes zero and sometimes not. In the moments of a non-zero rotational velocity, the vehicle is steerable and therefore controllable.

As a side effect of the first functionality, the ABS shortens the braking distance.
First of all, the slip λ is defined with the following function:

$$\lambda = 1 - \frac{\text{wheel speed}}{\text{vehicle speed}}$$

In words, a slip of 0% means a free rolling wheel, a slip of 100% means a completely locked wheel, and a slip of 20% means that while the vehicle travelled one meter, the wheels only rolled over 0.8 meters.
Figure 2.5 shows the relation between the friction coefficient and the wheel slip, and the relation between the steerability and the wheel slip. The friction coefficient depends on the wheel slip: for low slip the rolling friction is mainly acting, for higher slip, sliding friction becomes more dominant. The friction coefficient varies a lot between the different ground materials/ground conditions. The friction coefficient curve is based on empirical data, since it depends on the complex rubber tire behaviour.

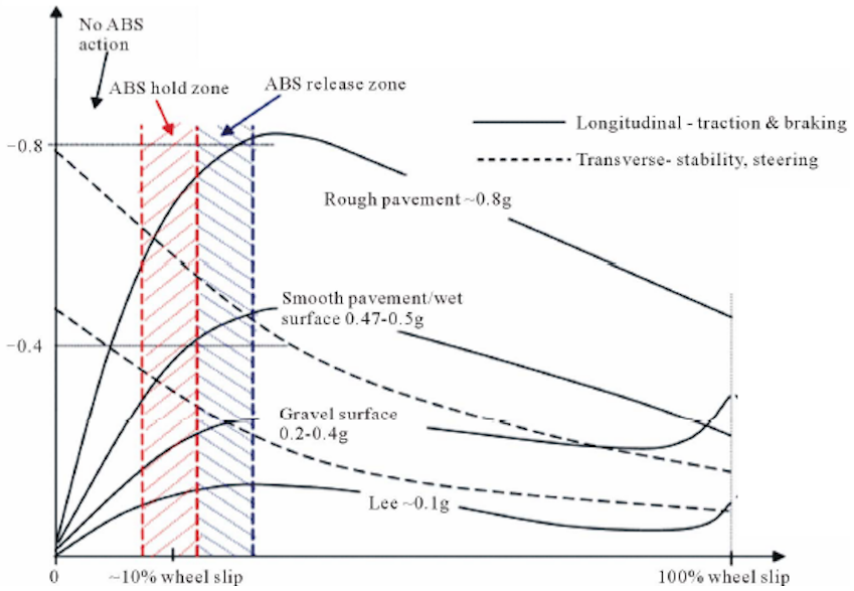

Figure 2.5: Illustration of the relationship between braking coefficient and wheel slip [15].

As a side effect to the ABS trying to keep the wheels from blocking in order to guarantee steerability, the slip is controlled to be in a range where the friction coefficient is high. A high friction coefficient leads to a shorter braking distance compared to normal braking where the wheel blocks completely and the slip is accordingly high.

The objectives for the ABS have been established based on the above explained theory:

- The ABS should **improve the steerability** of the go-kart during the braking process. By measuring the ratio of time during which the slip is under 25% to the whole duration of the braking process, the functionality of the ABS can be compared to a full braking without ABS.
- Comparing a full braking without ABS to a full braking with ABS, a **shortening of the braking distance** should be observed. The testing condition is given by the dry hangar ground and the regular go-kart tires.

Chapter 3

Methods

First, the go-kart specific units are defined. Then, the process of how the output is obtained from the corresponding input is presented for each ADAS. Within the scope of the "Studies on Mechatronics", a literature research for the EPS is realized.

3.1 Definition of the Units

3.1.1 SCT

SCT (Steering Column Torque) is the unit for torque used on the go-kart instead of newton meter. The unit SCT was introduced by the go-kart team because not enough information about the physical behaviour of the steering column actuator was provided by the manufacturer. There are two main applications for SCT:

- When the electric motor at the steering column has to apply a torque, the information about the amount of torque is transferred with the unit SCT.
- The torque applied by the driver at the steering wheel is measured in SCT. It is important to mention that the driver can apply a torque bigger than 1[SCT] at the steering wheel. However the sensor stops measuring after 1[SCT]. So, 1[SCT] applied torque is not the maximum torque that can be applied, but the maximum torque that can be measured.

In order to compare the torque values used on the go-kart to the torque values recommended in literature [Nm], a conversion function between the torque value τ [Nm] and the torque value T [SCT] has been established. Therefore, a force, which is increased in steps of 1 Newton, is applied at the steering wheel.

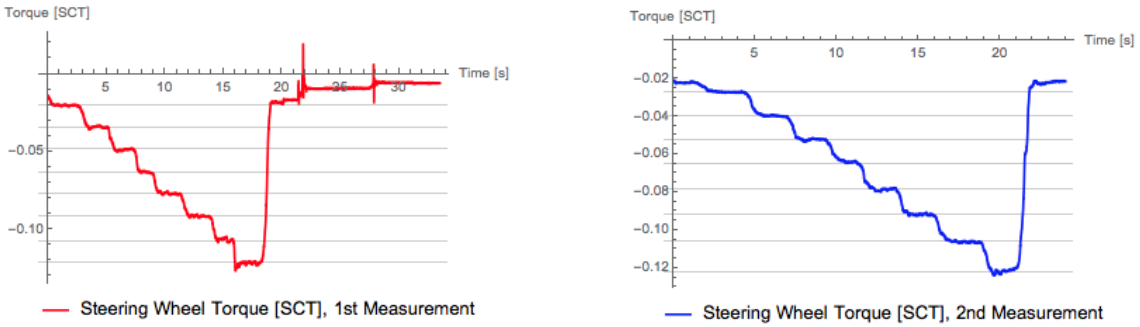

Figure 3.1: Measurements of the resulting torque step height for an increase in force of 1[N].

The resulting torque is measured at the steering column. The measured distance between the column and the point where the force applies is 0.134[m] (this measurement is a possible cause of error) and the force should be applied orthogonal to the distance (another possible cause of error).

Figure 3.2: Experiment set up.

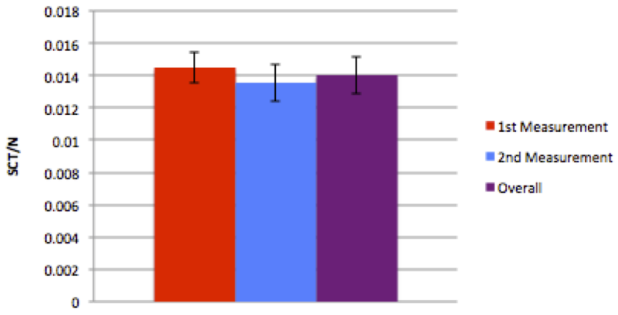

Figure 3.3: Resulting step height: [SCT/N]

The relation between the torque value τ [Nm] and the torque value T [SCT] is linear. The following applies:

$$0.01401[\text{SCT}] = 1[\text{N}] \cdot 0.135[\text{m}] = 0.135[\text{Nm}]$$
$$0.1045[\text{SCT}] = 1[\text{Nm}]$$
$$1[\text{SCT}] = 9.5638[\text{Nm}]$$

Positive torque turns into the mathematically positive direction and vice versa (see fig. 3.4).

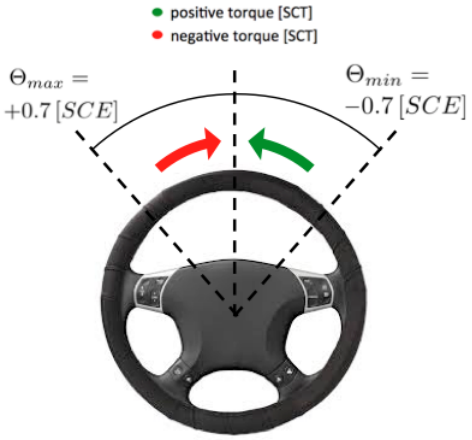

Figure 3.4: Introducing positive/negative position and torque direction.

3.1.2 SCE

SCE (Steering Column Encoder) is the unit used by the go-kart team for the angular position of the steering column, instead of angular degrees or radian measure. SCE have been introduced because the manufacturer did not provide the necessary information. The unit SCE can be converted into a more physically intuitive unit, the turning ratio [1/m]. This unit implies how much the vehicle turns (in radian measure) when 1 meter is travelled. The steer mapping from the SCE value ϵ to the turning ratio δ can be approximated with the following [16]:

$$\delta = 0.8284521034333863 \cdot \epsilon - 0.33633373640449604 \cdot \epsilon^3$$

The maximum steering angle is at ± 0.7[SCE], 0[SCE] implies no steering angle or going straight. A positive steering angle leads to heading towards the left-hand side (see fig. 3.4).

3.2 Electric Power Steering

3.2.1 Literature Review

The goal of the literature review was to examine papers with a focus on the different approaches to design an EPS. Most papers follow the division into "Steering System", "Torque Map" and "Controller", so the same structure is used for the review. As a result, a general method of how to design an EPS is outlined.
It was not possible to find research about an EPS done on a go-kart. So, as a first step, the main differences between the go-kart and the testing platforms used in the selected papers have to be highlighted.

- Cars have a rack and pinion steering system (see fig. 3.5) while the go-kart has a simpler steering system (see fig. 3.6). As a result, the force transmission is less uniform.
- On both, cars and go-karts, an accurate measurement of the actual front steering angle is hard to achieve. It is suggested to use the rack position [17] or the steering wheel angular position [18, 19] instead. On the go-kart and some papers [20], the steering column angular position is measured.
- None of the selected papers had the goal to eliminate the aligning torque since the return-ability was rated as a positive property. On the go-kart, return-ability is unwanted during autonomous driving due to its effect on the PID controller (refer to sec. 2.2). During manual driving, it depends on the driver's preferences whether return-ability is wanted or not.

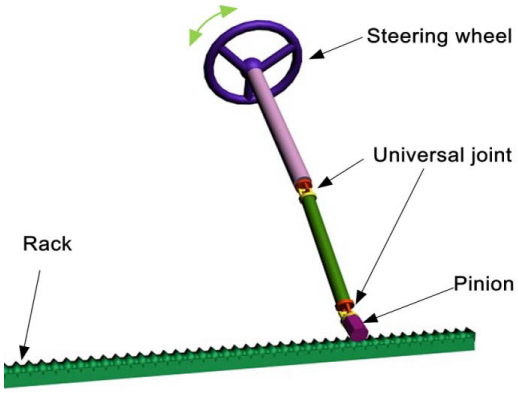

Figure 3.5: Manual steering configuration of a conventional car [21].

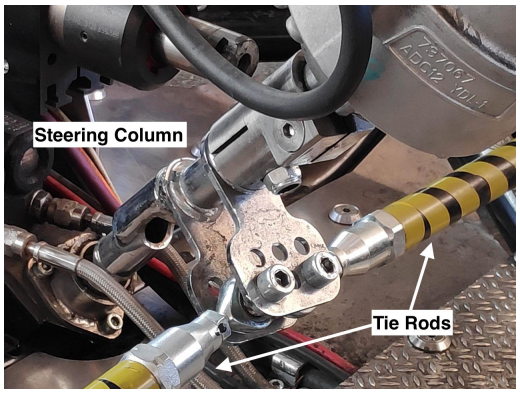

Figure 3.6: Steering configuration of the go-kart.

System Analysis and Modelling

As a first step, important components of an EPS are described. Then, the system as a whole is characterized and analyzed.

The main component of an EPS is the **electric motor**. Important properties of the electric motor are a smooth torque, high efficiency, minimum torque ripple, low inertia and weight. Most commonly, a DC motor is integrated into the steering system [22, 23, 20]. Three configurations of where the electric assist motor is mounted are widely used. These are column-type, mostly used

for small-sized cars, pinion-type for middle-sized cars and rack-type for trucks. The type depends on the weight of the vehicle [19, 24].

The **torque sensor** is another important component since the EPS depends on the steering wheel torque initiated by the driver as an input. Therefore, the torque sensor does not only have to measure accurately and with a high signal resolution, but has to be reliable in order to prevent an uncontrollable steering event. There exist many different types of torque sensors [25].

The steering system can be split up into three parts. The primary side includes all components starting from the steering wheel to the pinion driving rack. The steering gear consists of the steering rack connected to the electric motor. The third part is the front axle and the front wheel (see fig. 3.7).

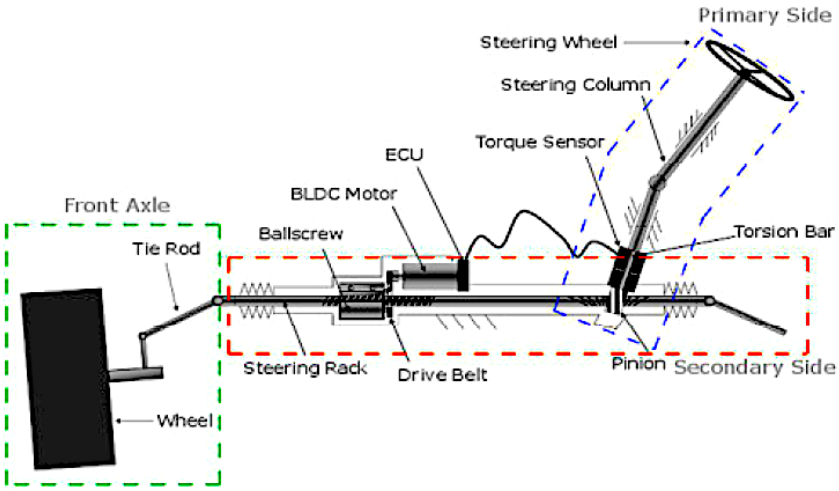

Figure 3.7: Overall description of the main steering system components [17].

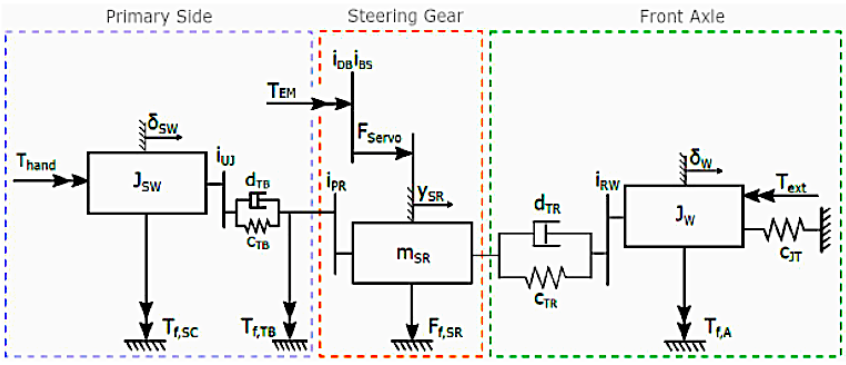

Figure 3.8: A possible model description of the steering system [17].

Most papers apply a model-based approach in order to develop the EPS. The **EPS dynamic model** interrelates the steering mechanism, the motor's electrical dynamics, and the tire/road contact forces. The model itself consists of four masses: the steering wheel, the column, the motor and the rack. The equation of mass can be set up accordingly to Newton's second law. As a result, a model in state-space form is obtained [23, 24, 19, 18, 22, 26]. However, the results differed from each other since different configurations (see electric motor) were chosen, and since different levels of complexity were aimed at.

An alternative way for achieving the state space representation is modelling the kinematic, potential and dissipative term and combining them within the Lagrange equation [17].

In order to obtain realistic models, it is necessary to consider the non-linearities of the steering system. Two important factors are the inherent friction within the steering system and the interaction between tire and ground. These can be modelled as viscous damping [17]. The variable gear ratio between pinion and rack, created by the varying spacing of the rack's teeth, is another non-linearity. (On the go-kart, this non-linearity is even more acting, see fig. 3.5) This effect is often linearised by assuming a constant gear ratio. The self-aligning torque resulting from the caster angle (refer to sec. 2.2) and depending on the vehicle velocity is also to mention as a non-linearity. In [22] the aligning torque is considered, in other models it is disregarded.

A **steering map** can be used to verify the quality of the steering model. In the experiment, a slalom curve is driven with constant velocity. The steering wheel angle Θ and the steering wheel torque T_d are measured and plotted versus each other. Modeling uncertainties are the reason for the gap between simulation and experiment.

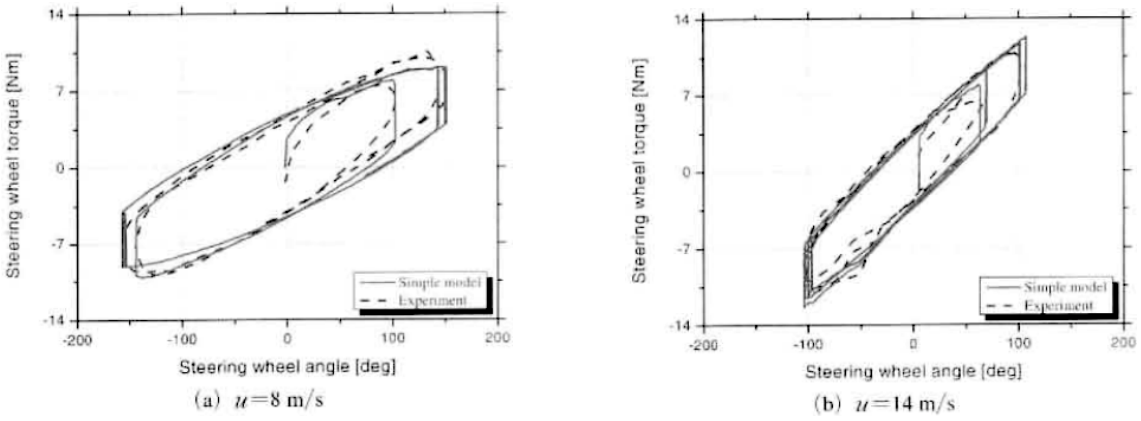

Figure 3.9: Steering wheel angle Θ vs. steering wheel torque T_d [22].

Torque Map

The torque map determines how much steering torque is assisted by the motor. It sets up the function between the measured torque applied by the driver and the assist torque applied by the motor. Therefore, the shape of the torque map defines how smooth the support from the EPS feels to the driver.

The straight-line boost curve is the most widely used torque map (used in [24, 23, 19]). Here, the assist torque is proportional to the applied torque, but depends on the current velocity of the vehicle. This type of assist map is calculated as following:

$$\mathrm{T}_m = \begin{cases} 0, & 0 \leq \mathrm{T}_d \leq \mathrm{T}_{d,0} \\ \mathrm{K}_V(v) \cdot (T_d - T_{d,0}), & \mathrm{T}_{d,0} \leq \mathrm{T}_d \leq \mathrm{T}_{d,max} \\ \mathrm{T}_{max}, & \mathrm{T}_{d,max} \leq \mathrm{T}_d \end{cases}$$

T_m	assist torque
T_d	steering wheel torque
$T_{d,0}$	steering wheel torque when assist torque begins to generate
$T_{d,max}$	steering wheel torque when maximum assist torque is applied
T_{max}	maximum assist torque
$K_V(v)$	coefficient depending on velocity

As a first step, the variables $T_{d,0}$ and $T_{d,max}$ can be obtained by experiments on the vehicle, since they depend on the feeling of the driver.
Then, the maximum steering resistance torque $T_{r,max,0}$ is measured while the vehicle has a velocity of 0 km/h. The maximum assistant torque for 0km/h can be calculated by the following equation.

$$T_{m,0} = T_{r,max,0} - T_{d,max}$$

The maximum steering resist torque is recorded under the velocity of 20[km/h], 40[km/h], 60[km/h], 80[km/h] and 100 km/h. The values found in the experiment set $T_{m,max,vel}$ for the corresponding velocity.
Taking these values as input, the slope of the boost curve can be calculated for each velocity and $K_V(v)$ can be found by using polynomial regression [23].

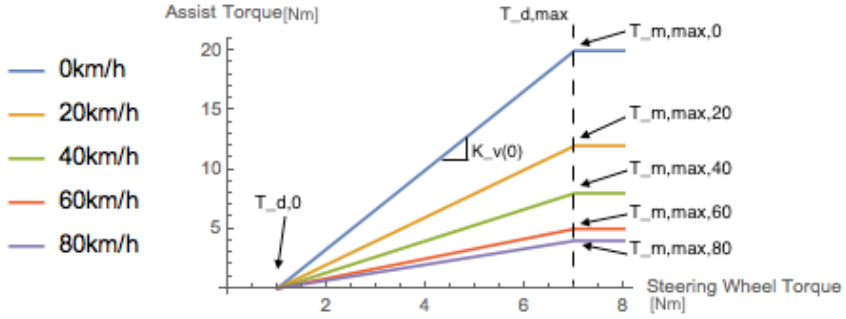

Figure 3.10: Straight line boost curve under different velocities.

The deadband under $T_{d,0}$ prevents the system from reacting too sensitively do the driver torque. As a disadvantage, this deadband adds another non-linearity to the steering system [24].

In some papers [21, 20, 26], more complex torque maps are used in order to describe non-linearities and eventually getting a better driving experience for the driver.

Controller Design and Evaluation

The **ECU (Electronic Control Unit)** computes the currently required assist torque based on the measured torque initiated on the steering wheel and on the velocity. This assist torque has to be applied by the electric motor, and the ECU controls the motor by feeding the corresponding current to the motor to generate the assist torque. Here, a suitable control system is necessary so that the actually applied assist torque matches the previously calculated assist torque [18].

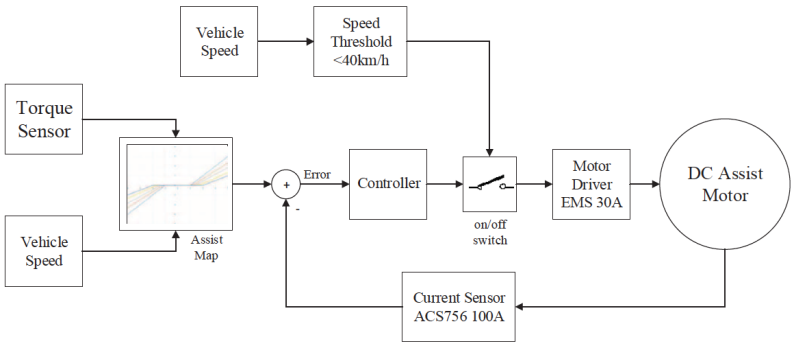

Figure 3.11: Description of the ECU used in [20].

In the following section, several different controllers are described and it is outlined, for what reason they are chosen.

In [18], an augmented observer and nonlinear damping controller are implemented. The damping controller suppresses the angle tracking error, while the observer estimates the full state and disturbance. It is necessary to estimate the disturbance, since the definition of the disturbance took into account friction, the non-linearities from the steering system and the torque applied by the driver. Therefore, the big modeling uncertainties in the disturbance are compensated by the implementation of the observer.

In [17], a linear system is assumed. The front angle controller is evaluated by looking at its trajectory-following ability. The controller is developed by pole placement and complemented with an LQI approach. In a first design attempt, weighting in the Q matrix is solely placed on the position and velocity of the rack position. With this, a good tracking performance of the front steer angle was achieved. However, it is observed that the steering wheel showed oscillatory behaviour during the rack position step response, so it gets necessary to put additional weighting to the steering wheel angle position and velocity within the Q matrix.

This paper [24] analyses the non-linear system and sets up stability conditions for the system afterwards. In order to fulfill them, a lead-lag compensator is employed. To ensure stability, it is necessary to increase the phase margin of the system by using a lead compensator. The lag compensator has to be added because the high frequency gain, a disadvantage of the lead compensator, has to be decreased to prevent noise amplification.

In [19], a PID controller was used . But instead of finding the PID parameters with conventional methods, a genetic algorithm optimization method was used to determine them. The genetic algorithm produces randomly many different sets of PID parameters, the first generation of parameters, and assigns to each set a fitness value accordingly to the quality of the set. Now, successive generations are created by combining and mutating the preceding generation. Sets of parameters with a higher fitness level are more likely to survive. Therefore, this is repeated until an optimal set of parameters is found.

Two remarks concerning the research on EPS controllers have to be done [24]:

- Some papers linearized the non-linear system for simplicity reasons. Linearized systems only describe the system accurately around the equilibrium point. Non-linear components of the system such as the torque map can cause divergent or oscillating behaviour.
- Just half of the papers actually tested their proposed controller on a real vehicle, but just in a simulation. Simulations don't take unmodeled parts of the system into account and they have difficulties to recreate complex influences such as the tire-road interaction.

Conclusion

The selected papers followed in general the same approach to design an EPS. Differing from paper to paper, the method used for the steering system analysis and the creation of a torque map are explained in different levels of detail.

When it comes to the question which controller should be implemented in an EPS, there is no consensus at all. Many different controllers are proposed. Comparing them with each other would require uniform testing conditions harmonized criteria.

3.2.2 Implementation

As a first attempt at a torque map, the straight line boost curve (see fig. 3.10) was implemented. But since the EPS has to compensate the aligning torque and at the same time reduce the torque the

driver has to apply, the straight line boost curve was not sufficient. Therefore, various experiments led to the implementation of the following torque map. The process of how it was created is described in this section.

$$T_m(\Theta, v_{lat}, T_d) = \underbrace{f(\Theta)}_{\substack{aligning\ torque \\ compensation\ term}} + \underbrace{c_1 \cdot v_{lat}}_{\substack{velocity\ dependent \\ compensation\ term}} + \underbrace{c_{2d}}_{driver\ support\ term}$$

T_m	assist torque applied by the electric motor
T_d	steering wheel torque applied by the driver
Θ	steering column angular position
v_{lat}	lateral vehicle velocity
v	vehicle velocity

Aligning torque compensation term

Due to the geometry of the go-kart (section 2.2), an aligning torque is acting on the steering column for every angle unequal zero. In order to compensate this aligning torque, three experiments were conducted with the goal to create a steering map based on data from the go-kart. More precisely, a function, which has the steering column angle Θ as an input and the torque T_d as an output, has to be established.

Figure 3.12: Set up of for the steering map experiments.

All three experiments were conducted with both front wheels placed on a surface with as little friction as possible (smooth paper fulfilled this requirement).

Experiment 1: A constant torque is applied. Then, the steering wheel is strongly deflected and returns to its equilibrium point after it is released.

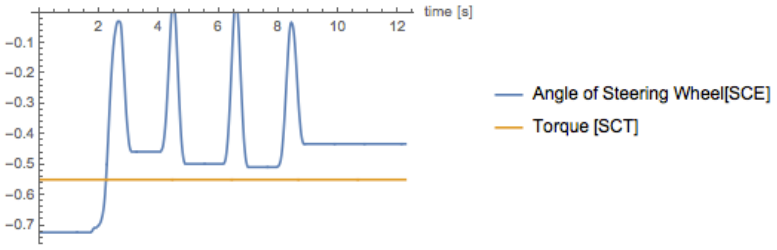

Figure 3.13: Plot example of experiment 1.

Experiment 2: The PID controller tries to keep a constant angle while the steering wheel is slightly deflected.

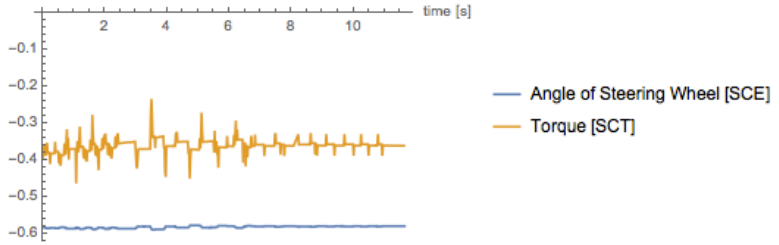

Figure 3.14: Plot example of experiment 2.

Experiment 3: Every torque between -0.7 and 0.7[SCT] is applied.

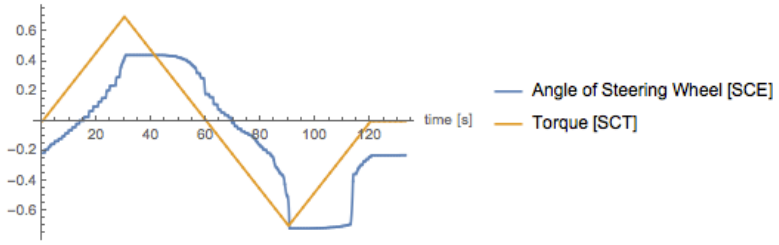

Figure 3.15: Plot example of experiment 3.

All data points, consisting of a torque value and a steering angle value, were fitted with a third-degree polynomial for each experiment. This led to five different possible aligning torque compensation functions. They were all tested on the go-kart by applying the calculated assist torque depending on the steering angle at slow velocity. The criteria was how good the function would keep an angle when no torque was applied by the driver.

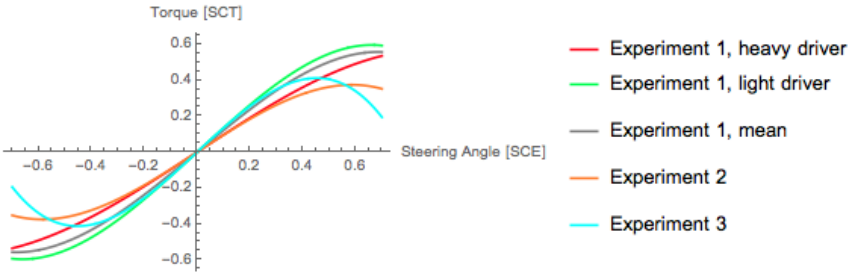

Figure 3.16: All possible aligning torque compensation functions.

The function from the second experiment (orange curve, see fig. 3.16) compensated the aligning torque the best, especially for large steering angles. The following function is the best approximation to map the steering angle Θ to the required torque T:

$$T_m(\Theta) = 0.958148 \cdot \Theta - 0.928108 \cdot \Theta^3$$

Velocity dependent compensation term

The aligning torque is created because the lateral velocity is not acting at a point on the steering column axis (see fig. 2.1). So, the magnitude of the torque depends on the lateral velocity. The aligning torque turns the steering wheel back towards the middle position. The impact of the aligning torque and it's dependency on the velocity is measured in the following experiment.

Experiment 4: A constant torque is applied. Then, the driver accelerates the vehicle and the deviation from the initial steering angle is measured.

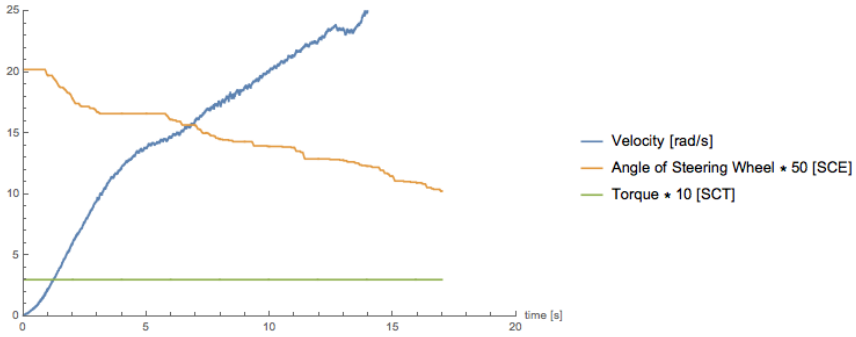

Figure 3.17: Plot example of experiment 4.

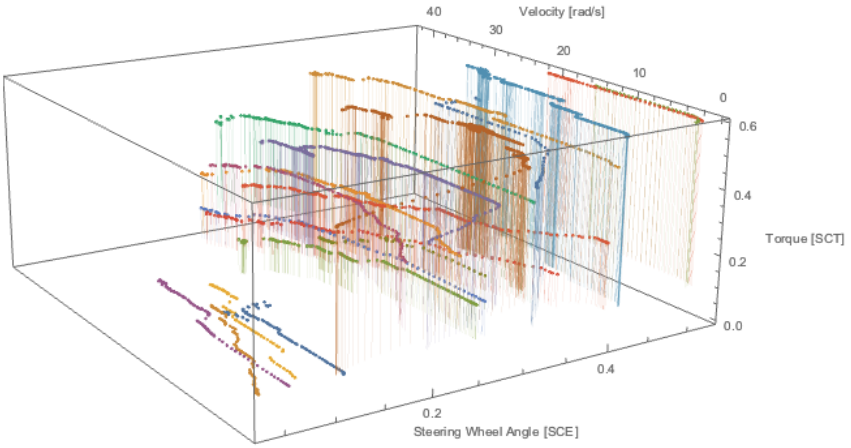

Figure 3.18: All executions of experiment 4 in one plot.

The values in figure 3.17 are scaled for presentiveness. Figure 3.18 shows, that for a constant torque, the steering angle is smaller for high velocities compared to low velocities.

Based on this result, a velocity dependent compensation term is introduced. The value for c_1 is found by experiments. The input values $v_{lat,right/left}$ have to be processed with an IIR (Infinite Impulse Response) filter to filter out the high frequency noise in the measurement.

$$T_m(v_{lat}) = 0.2 \cdot (v_{lat,\,right\,wheel} + v_{lat,\,left\,wheel})$$

Driver Support Term

When the assist torque applies the aligning torque compensation term and the velocity dependent compensation term, the go-kart is able to keep a steering angle, for constant velocities as well as for acceleration. However, the driver now has to apply a large driver torque in order to cause a change in steering angle. Figure 3.19 shows that the maximum driver torque of 1 [SCT] has to be applied several times in order to follow the track.

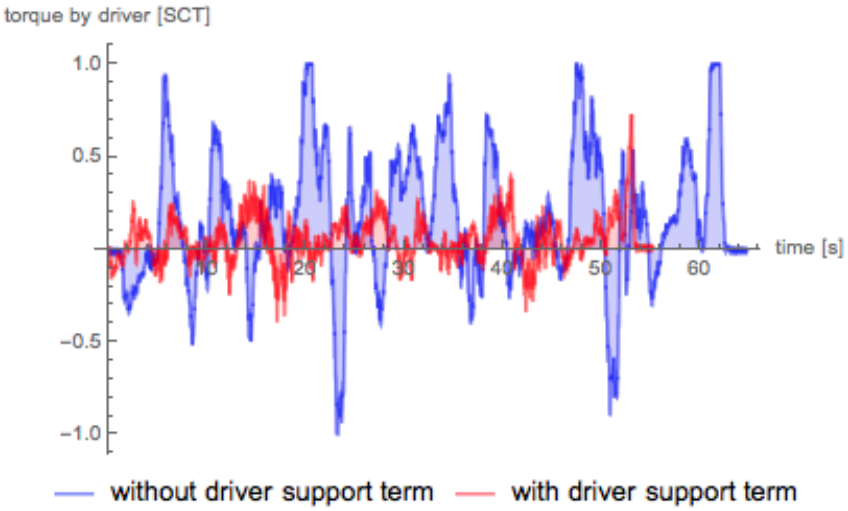

Figure 3.19: Comparison of the EPS with and without driver support term.

mode	distance [m]	total applied torque [SCT·s]	torque/meter [$^{\text{SCT}\cdot s}/_{\text{m}}$]
with driver support term	140.326	156.227	1.11331471
without driver support term	137.55	43.1974	0.31404871

Due to this, a driver support term has to be introduced.

$$T_m(T_d) = 0.8 \cdot T_d$$

The value for c_2 is found by experiment, too. A too high value would make the steering system too sensitive for the movements on the steering wheel, and unintentional movement on the steering wheel would be amplified. With a too low value, the EPS would not fulfill the goal of reducing the steering effort of the driver.

Boundedness

The assist torque has to be bounded due to safety reasons. Otherwise, extreme driving situations could provoke a huge assist torque which would worsen the situation. Therefore, the terms are limited if necessary:

$$\begin{aligned} T_m(\Theta, v_{lat}, T_d) = & \underbrace{0.958148 \cdot \Theta - 0.928108 \cdot \Theta^3}_{\textit{aligning torque compensation term}} && \text{for } -0.7 < \Theta < +0.7 \\ & + \underbrace{max(0.2 \cdot (v_{lat,\,right\,wheel} + v_{lat,\,left\,wheel}),\, 0.5)}_{\textit{velocity dependent compensation term}} \\ & + \underbrace{0.8 \cdot T_d,}_{\textit{driver support term}} && \text{for } -1.0 < T_d < +1.0 \end{aligned}$$

$$
\begin{aligned}
T_{m,max}(\Theta_{max}, v_{lat,max}, T_{d,max}) \; = \\
& 0.958148[\mathrm{SCT/SCE}] \cdot 0.7\,[\mathrm{SCE}] - 0.928108[\mathrm{SCT/SCE^3}] \cdot (0.7[\mathrm{SCE}])^3 \\
& + 0.5[\mathrm{SCT}] \; + \; 0.8 \cdot 1.0[\mathrm{SCT}] \\
& = 1.6523[\mathrm{SCT}]
\end{aligned}
$$

So, the assist torque is bounded to its maximum value of ± 1.6523[SCT].

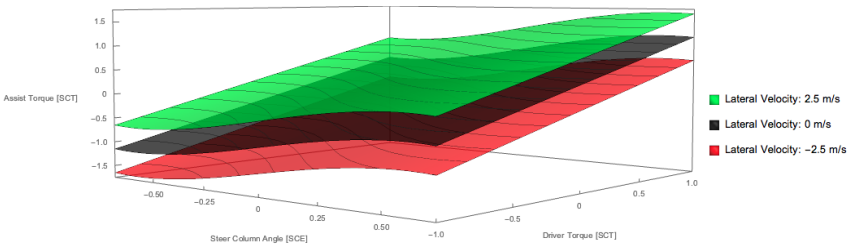

Figure 3.20: Analysis of the unwanted steering wheel vibration.

Adjustment

The previously explained implementation was tested on the go-kart. An issue which turned up was a vibration of the steering wheel. The vibration had a high frequency but low torque, so it could be stopped by applying a small force at the steering wheel.

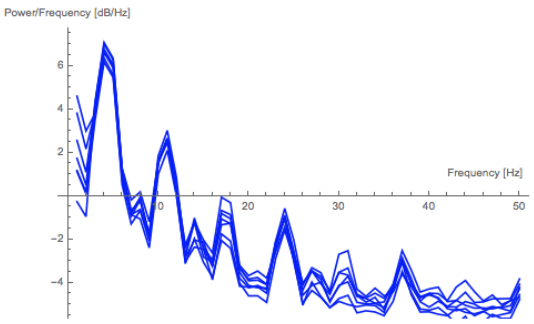

Figure 3.21: Power spectrum of the torque measured at the steering wheel T_d.

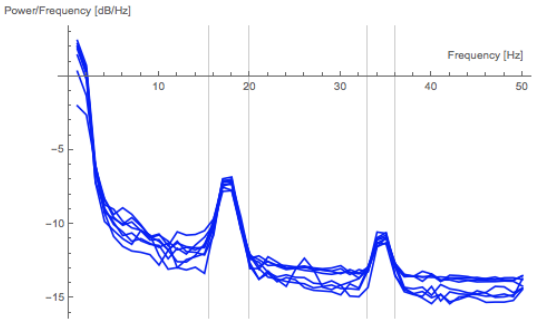

Figure 3.22: Power spectrum of the steer column angular position.

Figure 3.21 and figure 3.22 were created by plotting the squared magnitude of the discrete Fourier transform (power spectral density) of the list of the torque applied at the steering wheel respectively the list of steering column angles. For this purpose, the steering wheel vibration was provoked and logged several times. The driver applied no torque during the vibration. Therefore, the measured torque at the steering wheel comes from the inertia of the steering wheel. Conceiving the EPS as a controller, it has high frequency eigenvalues which are not damped. If the input (torque measured at the steering wheel) excites the system with its resonance frequencies, the system starts oscillating.

In order to prevent the vibration, an IIR filter is implemented in the driver support term to filter out the high frequencies of the measured driver torque T_d. This adjustment in the implementation of the EPS was effective; it is not possible to provoke the vibration anymore, nor did it happen spontaneously during test drives.

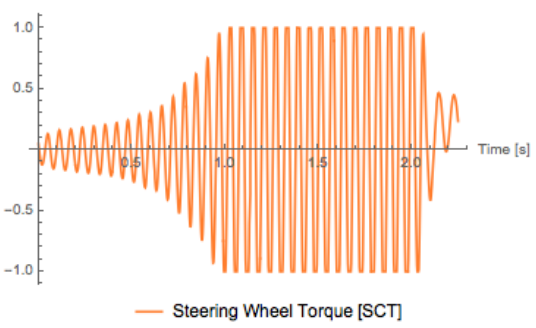

Figure 3.23: Steering wheel torque without the filter implementation. The amplitude diverges up to the maximum torque. Then, the torque is stopped by the driver.

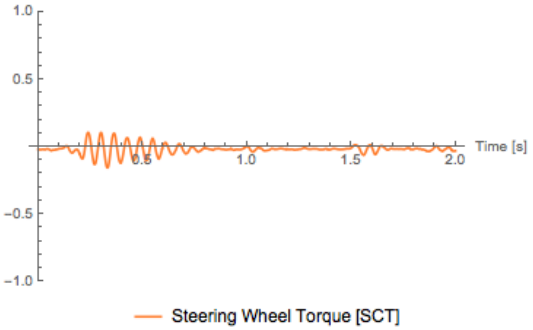

Figure 3.24: Steering wheel torque with the filter implementation. The amplitude starts to oscillate. Previously, this would have diverged, but now it is damped by the EPS.

3.3 Lane Keeping Assist

3.3.1 Implementation

Lane Design

In conventional lane keeping assist systems, the lane is detected based on data of a realtime camera. Then, a lane detection algorithm identifies the lane on the images. Since implementing a lane detection algorithm is complex and time consuming, the lane needed in the lane keeping assist implemented for this thesis is designed by the driver and then provided as an input to the lane keeping assist.

A sequence of control points are chosen as an input. The centerline curve is generated by refining the sequence using the Lane-Riesenfeld subdivision algorithm [27]. A good animated explanation of this algorithm is published here: [27]. The resulting limit curve consists of piecewise clothoid approximations.

"A clothoid is a curve whose curvature changes linearly with its length."[28] Clothoids are often used to design the curve of a section of highway or railroad. They are applied because they prevent the vehicle form experiencing a sudden centripetal acceleration. For the same reason, clothoids are implemented in the path planning code of the go-kart.

Left- and right-hand to the previously generated centerline, lane boundaries in an adjustable distance are added.

Allowed Steering Range

For each position on the lane/next to the lane, the maximal and minimal steering ratio (rotation/meter [$^1/_m$]) is calculated.
First, a point which is within the look ahead distance and on the left/right lane boundary, is determined. Next, the clothoid, that will lead to this point the fastest, is planned. From this clothoid, the needed steering ratio to follow the clothoid, is derived. If this is done for both, the left and right lane boundary, a maximum and a minimum steering ratio are obtained. If the go-kart is on the lane, it will stay on the lane if the applied steering ratio is within the allowed range of steering ratios. If the go-kart has already left the lane, it will return to the lane, if a steering ratio, which is within the allowed range, is applied. Figure 3.25 shows the planned clothoids in bright red and bright green.

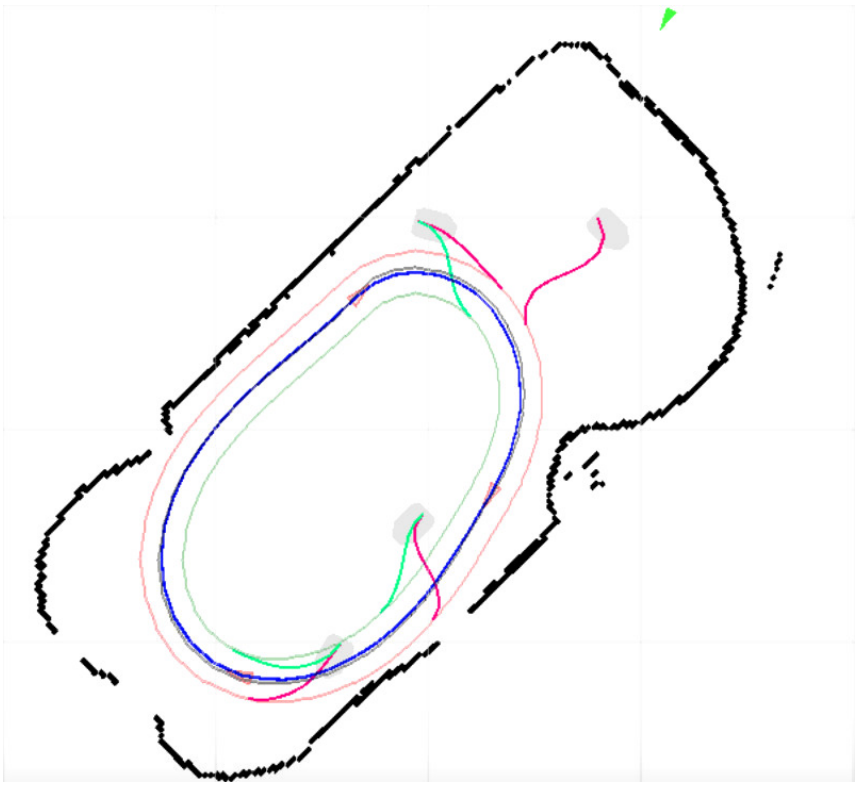

Figure 3.25: Design of the lane. Additionally, several visualizations of the maximum/minimum steering ratio are displayed.

Assist Torque

Same as for the EPS, a torque map has to be created as a lookup table for the assist torque. Within the allowed steering range, no assist torque is applied, except for the assist torque from the EPS. Outside the steering range, the assist torque is applied, depending on how big the difference between the current steering range and the allowed steering range is. This leads to a gentle intervention in the beginning of an assist torque operation. The assist torque is bounded to a limit of 0.8[SCT]. This allows the driver to leave the lane when he intends to, since the steering torque applied by the driver has its maximum at 1[SCT]. Therefore, the driver is always in charge of steering.

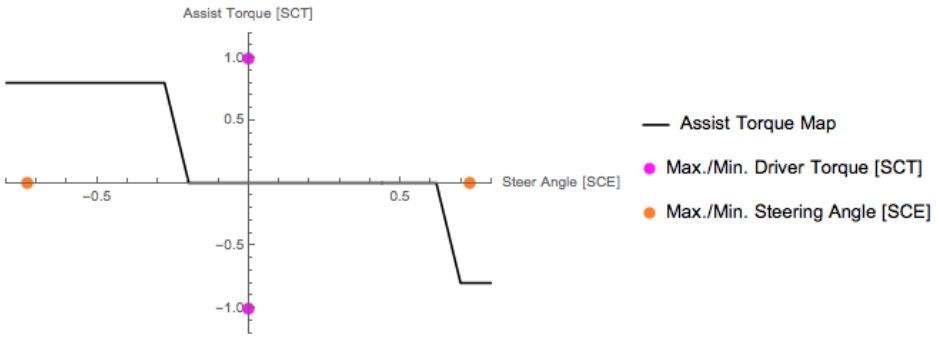

Figure 3.26: Assist torque map for the lane keeping assist. It depends on the currently allowed steering range.

Fig. 3.27 shows the planned steering range boundaries for a driving situation, where the go-kart has left the lane. The driver is allowed to steer to the left almost with the maximum steering angle of 0.7[SCE] since this will lead him back to the lane. He is not allowed to steer further to the right than -0.19[SCE].
The torque assist map for this situation is shown in figure 3.26.

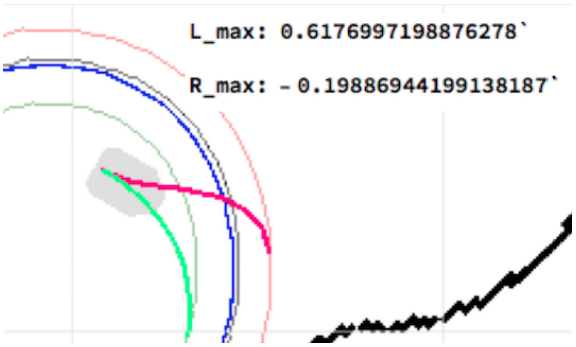

Figure 3.27: Planning of the steering range.

3.4 Anti-lock Brake System

3.4.1 Implementation

On the go-kart, two electric linear motors are mounted, one at each rear wheel. These linear motors are responsible for pressing the brake chocks onto the wheel in order to actuate the braking process. The position variable of both linear motors is referred to by x_n. There is just one position variable for both wheels, so the left and right linear motors have the same position.

The slip coefficient is calculated accordingly to section 2.4:

$$\lambda = 1 - \frac{\text{wheel speed}}{\text{vehicle speed}} = \text{vehicle speed} - \text{wheel speed}$$

The vehicle speed is measured by reading out the lidar data. The wheel speed is calculated by measuring the angular velocity of the rear wheel and multiplying it with the radius of a rear wheel. The slip coefficient calculation is implemented in the go-kart code as the rearrangement on the right, since a division by zero has to be prevented. By calculating the slip coefficient, a measure for the blocking of the wheel is obtained.

An ABS is responsible for controlling the brakes. The input to the controller are the two current slip coefficients. As soon as the maximum slip is exceeded on one wheel, the gap between the brake chocks and the wheel is extended. This way, the blocking of the wheel is released and the slip will decrease. The same procedure is triggered when the minimum slip is deceeded.

$$x_{n+1} = \begin{cases} x_n - \Delta x, & (\lambda_1 \,\text{OR}\, \lambda_2) > \lambda_{max} \\ x_n, & \lambda_{min} < (\lambda_1 \,\text{AND}\, \lambda_2) < \lambda_{max} \\ x_n + \Delta x, & (\lambda_1 \,\text{OR}\, \lambda_2) < \lambda_{min} \end{cases}$$

$\lambda_{max/min}$	slip range, where the friction coefficient is at a max
λ_1	slip coefficient of left rear wheel
λ_2	slip coefficient of right rear wheel
Δx	small step to adjust the brake position
x_0	initial brake position at the beginning of the full braking process
x_n	current brake position, $0 < x_n < 1$
x_{n+1}	future brake position, $0 < x_{n+1} < 1$

Experiment 5: The variables Δx and $\lambda_{max/min}$ are found in experiments. The go-kart is accelerated, then, a full braking is performed with one set of parameters. This is repeated several

times for every set of parameters. In the following evaluation, the braking distances are compared in order to find the best parameters.

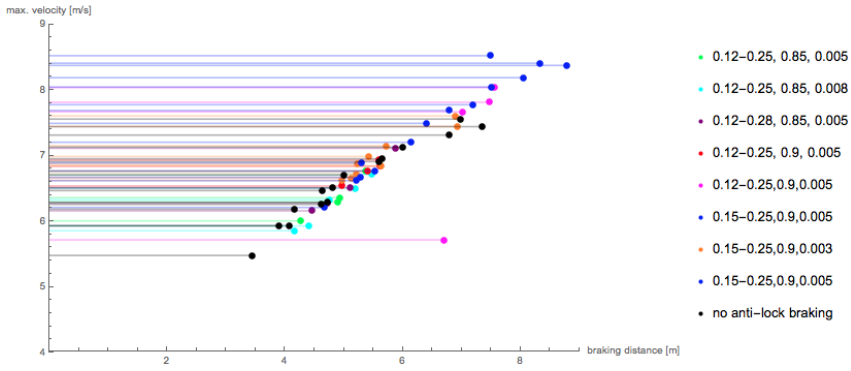

Figure 3.28: Some repetitions of experiment 5. The numbers in the plot legend stand for [λ_{min} - λ_{max}, x_0, Δx].

The experiment is repeated with the sets of parameters that performed good. Eventually, the following parameters are found to be the best parameters, concerning braking distance:

$$\begin{aligned} x_0 &= 0.9 \\ \lambda_{min} &= 0.15 \\ \lambda_{max} &= 0.25 \\ \Delta x &= 0.003 \end{aligned}$$

Chapter 4

Results

All experiments have been conducted on the go-kart testing platform described in section 2.1. Example plots are shown in this chapter, the plots of the complete recording are attached in the appendix A.

4.1 Electric Power Steering

4.1.1 Reduce Steering Torque

The main goal of the EPS is the improve the driving experience of the driver. The EPS supports the driver in his task to steer by applying an assist torque. To quantify the effectiveness, the applied torque per meter is measured with and without EPS. In a perfect experiment, one would compare the exactly same drive with and without EPS. But since this is not possible, it is tried to repeat the drives as similar as possible. Additionally, a large distance (5672[m]) is evaluated in order to provide comparability.

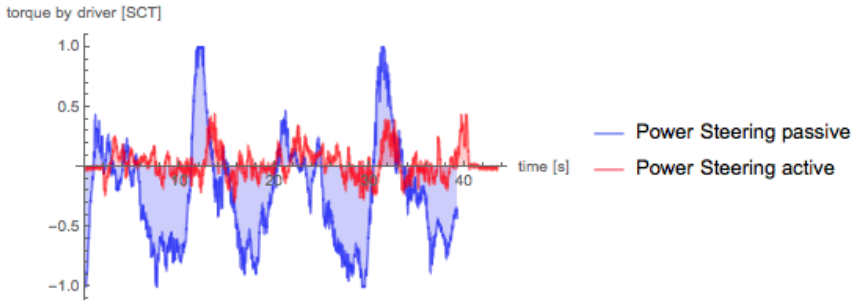

Figure 4.1: The same track is driven with and without EPS. The applied driver torque is measured and compared.

The experiment is conducted on three different tracks: a circle-shaped track, an eight-shaped track, and a random racing track. Additionally, the experiment is repeated for three different velocity categories: slow ($v_{mean} < 2.5[\mathrm{m/s}]$), medium-speed ($2.5[\mathrm{m/s}] < v_{mean} < 3.5[\mathrm{m/s}]$) and fast ($3.5[\mathrm{m/s}] < v_{mean}$). The plots of the experiment are displayed in the appendix A.1.1.

The ratio ρ of the applied driver torque with EPS to the applied driver torque without EPS is calculated for each repetition. The results are displayed in table 4.1. The mean, standard deviation and the ratio of the standard deviation to the mean (CV, coefficient of variance) are displayed below. **Overall, the mean is 27.282%, the standard deviation is 5.275% and the CV is 0.193.** Table 4.1 shows the trend that for slow velocities, the driver torque reduction is higher than for fast velocities.

	ρ		
	slow	medium	fast
circle-shaped	17.946%	22.336%	32.898%
circle-shaped	26.473%	34.747%	26.414%
eight-shaped	21.714%	29.314%	29.690%
eight-shaped	19.764%	30.538%	33.269%
racing track	28.599%	23.117%	32.414%
mean μ	22.899%	29.234%	30.568%
standard deviation σ	4.501%	5.153%	3.201%
CV	0.196	0.176	0.104

Table 4.1: Results of the ratio of the applied driver torque with EPS to the applied driver torque without EPS.

4.1.2 Compensate Aligning Torque

One of the two goals of the EPS was to compensate the aligning torque. If this succeeds, the go-kart should be able to keep a steering angle, provided that no torque is applied. Therefore, to make this objective quantifiable, the average deflection per meter is measured when no driver torque is applied. This is repeated several times with and without EPS.
Deflection is defined as positive when the steering wheel turns towards the middle. For calculating the average of the deflection, the absolute value of the deflection is taken.

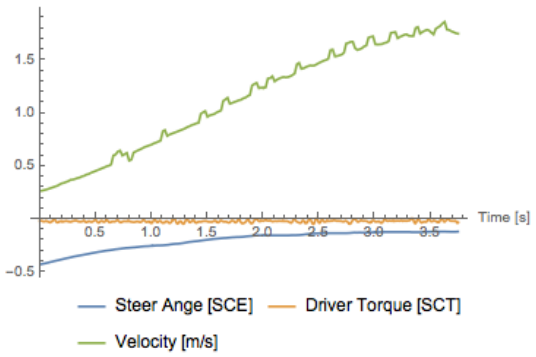

Figure 4.2: A test drive without an applied driver torque, and without EPS.

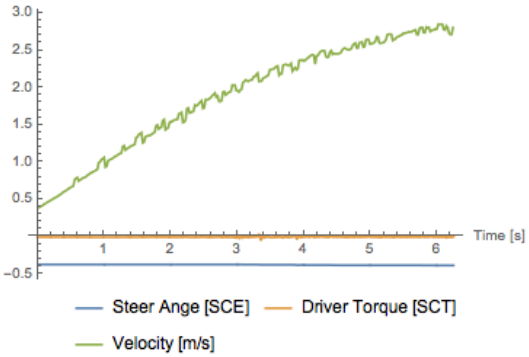

Figure 4.3: A test drive without an applied driver torque, but with EPS.

Figure 4.2 shows how the steering wheel is turned back solely by the aligning torque.
Table 4.3 shows the results of the test series where the deviation per meter was measured. **The average deflection per meter while driving with EPS is only 4.8% compared to the deflection per meter without EPS.**
In the appendix A.1.2, all plots from the aligning torque experiment are displayed, in the same order as in the table.

	deflection/meter		
EPS on/off	mean μ	standard deviation σ	CV
off	0.039404124	0.017118864	0.434443475
on	0.001949277	0.001048111	0.537692053

Table 4.2: Evaluation of the deflection per meter based on the results of table 4.3

EPS on/off	deflection [SCE]	distance [m]	max.velocity [m/s]	deflection/meter
off	0.18	6.140	1.020	0.0293
off	0.292	4.244	1.749	0.0687
off	0.147	5.096	2.086	0.0288
off	0.152	5.116	2.124	0.0297
off	0.161	3.988	2.427	0.0403
on	0.014	4.447	2.127	0.0031
on	0.005	6.655	1.963	0.0008
on	-0.015	5.675	2.791	-0.0027
on	-0.012	11.780	2.804	-0.001
on	0.013	6.249	3.325	0.0021

Table 4.3: Results from the aligning torque experiment.

4.1.3 Discussion

While driving with an active EPS, the driver just needs to apply one fourth of the driver torque. The reduction is mainly due to the driver support term (refer to sec. 3.2.2). It is a possibility to increase the driver support coefficient for more support. A side effect that would turn up is the increased sensitivity of the steering system: even slight, unintended movements on the steering wheel would be amplified by the EPS. Hence, the steerability would decrease.

The EPS compensates the aligning torque really well, the small deflections that still occur are negligible.
The driver torque curve is in general less vibrant in test drives with EPS compared to test drives without EPS (fig. 4.2 vs. fig. 4.3). The EPS stabilizes the swinging of the steering wheel.

In general, an EPS and the corresponding parameters, especially the driver support term, depend a lot on the driver's habits and expectations. Some drivers prefer driving without EPS in order to have a better feeling for the steering system, others wish as much support as possible. The same goes for the aligning torque: Whether an aligning torque is desirable or not depends on the field of application: a normal car needs an aligning torque during high speed driving in order to prevent accidents, on the go-kart the aligning torque was more of a disturbance than a help. So, before implementing an EPS, it is necessary to determine the requirements exactly.

4.2 Lane Keeping Assist

4.2.1 Keep the Driver on the Lane

If the driver is about to leave the lane by applying a medium driver torque (< 0.8[SCT]), the lane keeping assist should keep him on the lane. In order to evaluate this, 577[m] are driven with the lane keeping active, on different tracks. During these test drives, the maximum error (distance between go-kart position and lane boundary (not lane centerline)) was **0.755[m]**. The applied driver torque that provoked this error was 0.661[SCT]. Higher driver torques were observed during

the test drives, but never caused such a big error. The reason for this is that the relatively high driver torque was applied while the go-kart was driving at a high speed.

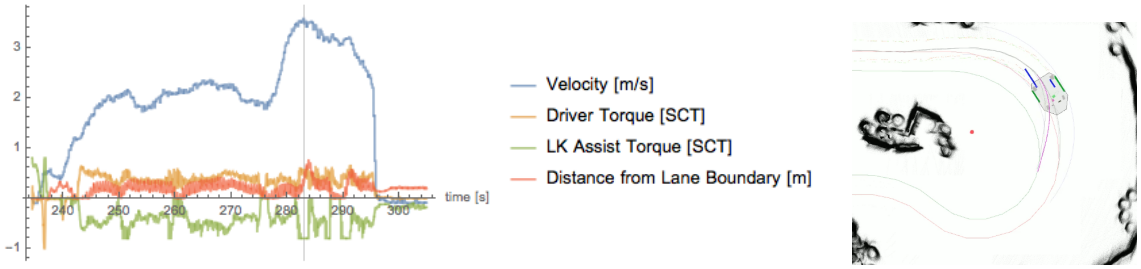

Figure 4.4: Appearance of the biggest error among the evaluated data, while the maximum applied driver torque is smaller than 0.8[SCT]

When no driver torque is applied, the go-kart should not leave the lane. This experiment was conducted on 243[m], as well on different tracks. The maximum distance from the lane boundary that was measured was **0.13[m]**.

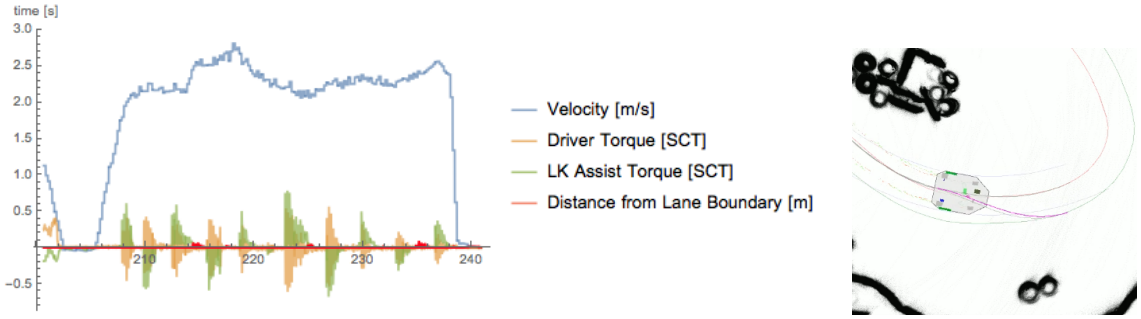

Figure 4.5: No driver torque is applied. The maximal distance between the go-kart position and the lane boundary is 0.080[m].

4.2.2 Driver stays in Control

The lane keeping assist can not force the driver to stay on the lane. If the driver wants to leave the lane intentionally by applying a high driver torque (> 0.8[SCT]), the lane keeping assist can not enforce him to stay on the lane. Figure 4.6 shows how the driver applies the torque just for a short duration of time. This is enough to overpower the assist torque.

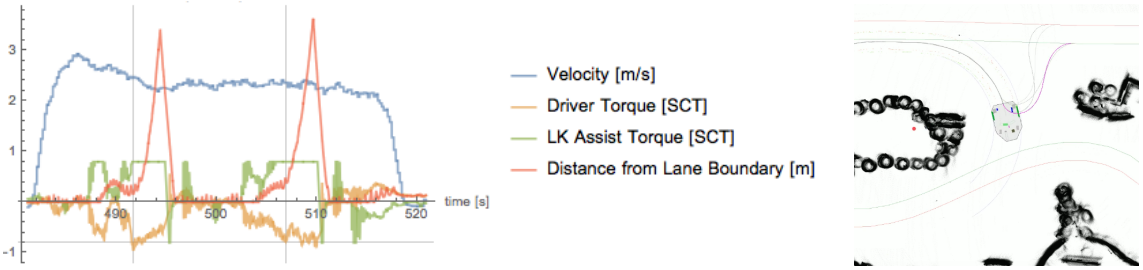

Figure 4.6: A torque higher than 0.8 [SCT] is applied at the steering wheel. This enables the go-kart to leave the lane.

4.2.3 Smooth Steering

Section 3.2.2 describes how the IIR filter is implemented in the EPS. This improvements was necessary since the observed oscillation of the steering wheel occurred close to every time when the lane keeping assist had to lead the vehicle back to the lane. As a consequence, the goal of smooth steering is registered.
It was possible to provoke the oscillation by first applying a high driver torque which causes the lane keeping assist to counteract with the maximal assist torque. If the driver then suddenly releases the steering wheel, the assist torque is still applied with the aim to lead the go-kart to the lane and therefore starts the oscillation. Figure 4.7 shows this process of deflection and release before the IIR filter was implemented in the EPS, figure 4.8 afterwards. In both cases, the go-kart returns to the lane, but once with an oscillating steering wheel and once with smooth steering movement. The displayed power spectral density diagrams show how the high frequency oscillation is damped.

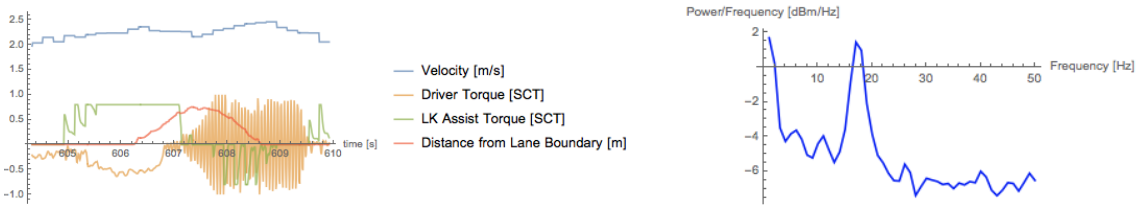

Figure 4.7: A plot of how the go-kart is led back to the lane by the lane keeping assist. As a side effect, oscillation occurred. On the right, the corresponding power spectral density diagram is displayed.

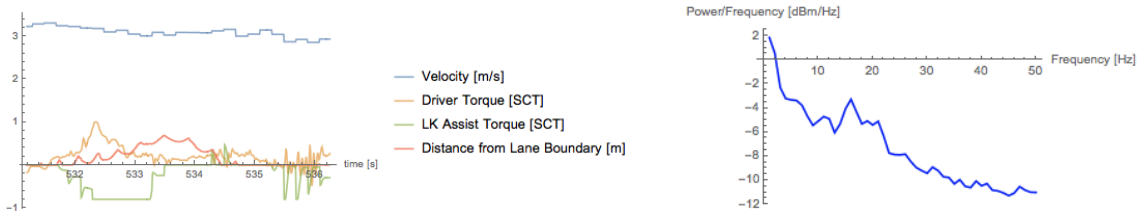

Figure 4.8: A plot of how the go-kart is led back to the lane by the lane keeping assist with smooth steering movements. On the right, the corresponding power spectral density diagram is displayed.

4.2.4 Discussion

The current implementation of the lane keeping assist achieved the objectives that were set in the subsection 2.3 for velocities smaller than 3 [$^{m}/_{s}$]. For higher velocities it was observed that the go-kart can leave the lane even though the applied driver torque is smaller than 0.8[SCT]. A possible attempt to solve this issue could be a velocity dependent maximum assist torque. Due to the time limitation, the further development of the lane keeping assist is left for future work.

A variation of the lane keeping assist could be an "invisible fence" within the testing area. When the maximal assist torque of the lane keeping assist is increased to a value > 1[SCT], the lane keeping assist will always be stronger than the driver. So, it can force the driver to stay in a given area. When the driver tries to leave, he is gently led back to the allowed area. First experiments are already conducted with an increased maximum assist torque, but further effort would be needed to set up such a feature.

4.3 Anti-lock Brake System

4.3.1 Braking Process with and without ABS

Comparing the plots shows the differences between a full braking with active ABS vs. passive ABS (see fig 4.9 and fig. 4.10). Without ABS, the wheels block completely, so the slip is most of the time 1, while the angular velocity of the wheels is often close to zero. In contrast, with ABS, the brake position adjusts in order to deblock the wheels if necessary. The wheel turning rate is most of the time unequal zero which makes the vehicle steerable.

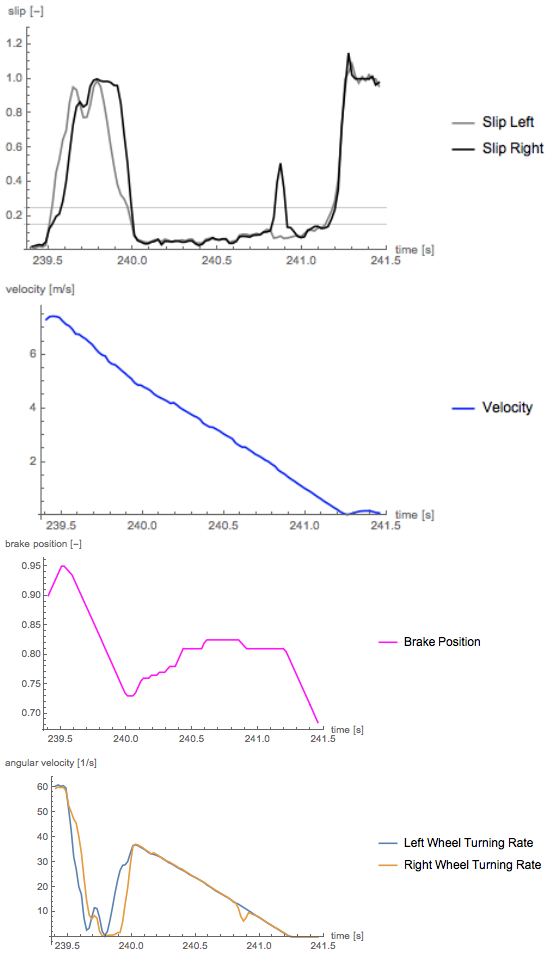

Figure 4.9: Braking process with ABS active.

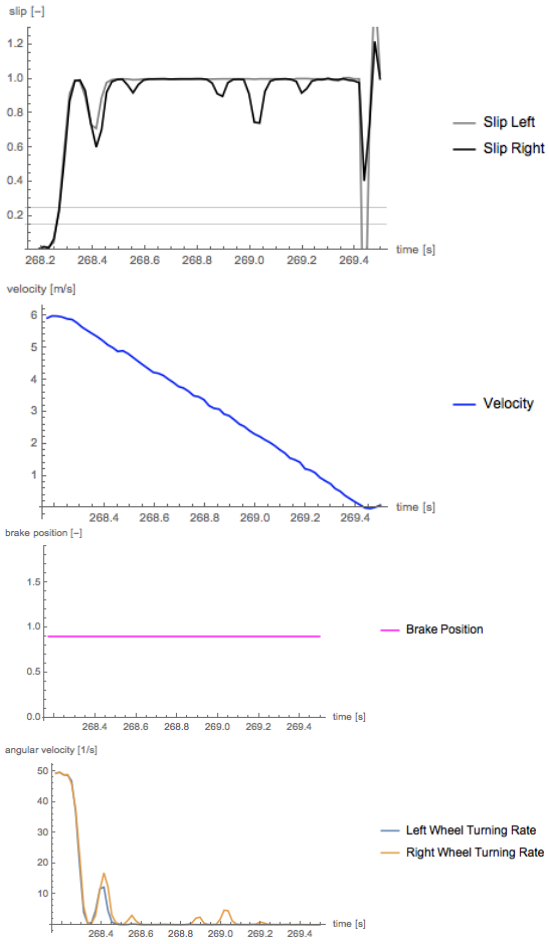

Figure 4.10: Braking process with ABS passive.

4.3.2 Improvement of the Steerability

The go-kart is steerable when the rear wheels are not blocked, so that the translational velocity still can be adjusted. To ensure steerability, a slip smaller than 25% is needed.
The improvement of the steerability is measured by the following experiment: The go-kart is accelerated, then a full braking is conducted. This is repeated several times, especially for different velocities, with and without ABS. Based on the logfile data, the time during which the slip was under 25% is compared to the whole braking process time. The characteristic values are defined below:

v_{max} [m/s]	maximum velocity at the beginning of the braking process
d_b [m]	braking distance
t_{tot} [s]	total time of the braking process
$t_{\lambda<0.25}$ [s]	time of the braking process, during which the slip is smaller than 25%
ratio ρ [−]	steerability ratio of $t_{\lambda<0.25}$ to t_{tot}

The characteristic values are obtained for every repetition. Based on this results, the average and the standard deviation are calculated. For a better intuition, the ratio of the standard deviation to the average, the coefficient of variation (CV), is added.

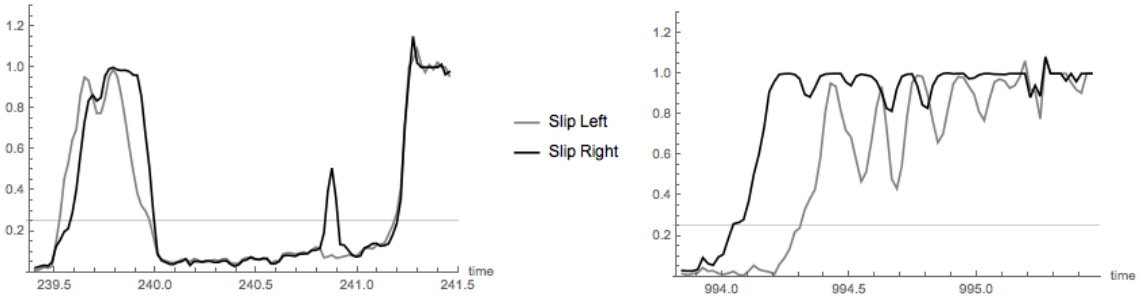

Figure 4.11: Example plots of a braking process with (left) and without (right) ABS. Slip under 0.25 provides steerability.

Table 4.12 shows, that **the steerability ratio with ABS is 1.89 times the steerability ratio without ABS.**

	ABS on/off	mean μ	standard deviation σ	CV
v_{max}	on	6.750	0.746	0.110
d_b	on	5.481	1.414	0.257
t_{tot}	on	1.653	0.282	0.171
ratio ρ	on	0.463	0.119	0.258
v_{max}	off	6.389	0.862	0.135
d_b	off	4.757	1.266	0.266
t_{tot}	off	1.573	0.171	0.108
ratio ρ	off	0.245	0.229	0.935

Figure 4.12: Average, standard deviation and the CV of the characteristic values with and without ABS (based on the results of table 4.13 and table 4.14).

v_{max}	d_b	t_{tot}	$t_{\lambda<0.25}$	ratio ρ
6.624	4.906	1.639	0.858	0.523
7.149	5.648	1.543	0.842	0.545
6.871	5.163	1.623	0.862	0.531
6.556	5.149	1.645	0.603	0.366
6.986	5.355	1.603	0.860	0.536
7.319	6.859	2.051	1.407	0.685
6.785	5.571	1.749	1.286	0.735
7.453	6.819	2.325	1.142	0.491
7.238	6.070	1.949	1.367	0.701
6.971	5.310	1.581	0.598	0.378
5.691	3.642	1.262	0.441	0.349
5.105	3.005	1.282	0.302	0.235
5.221	3.294	1.405	0.341	0.243
6.042	4.265	1.347	0.542	0.402
5.816	4.061	1.544	0.380	0.246
6.153	4.330	1.588	0.522	0.329
5.792	3.883	1.544	0.482	0.312
5.964	4.199	1.345	0.503	0.373
6.209	4.538	1.327	0.541	0.407
6.786	5.646	1.564	0.743	0.475
6.260	4.443	1.424	0.582	0.409
6.305	4.783	1.428	0.603	0.422
6.641	4.894	1.386	0.561	0.405
6.298	4.696	1.407	0.643	0.457
6.2172	4.490	1.488	0.642	0.431
7.174	5.575	1.584	0.743	0.469
7.245	5.933	1.527	0.725	0.475
7.089	5.821	1.744	0.863	0.494
7.055	9.728	2.370	1.263	0.533
7.937	7.947	1.963	0.841	0.428
8.063	7.659	2.083	1.103	0.529
7.585	6.745	1.664	0.882	0.529
7.823	7.359	2.126	1.082	0.509
7.569	6.476	1.688	1.064	0.630
7.640	6.746	1.825	1.004	0.550
7.360	6.321	1.872	0.986	0.526

Figure 4.13: Results of examining the braking process with ABS.

v_{max}	d_b	t_{tot}	$t_{\lambda<0.25}$	ratio ρ
3.889	1.761	1.286	0.141	0.110
5.885	3.855	1.307	0.865	0.661
6.111	4.105	1.466	0.160	0.109
5.669	4.176	1.625	0.301	0.185
5.444	3.384	1.423	0.279	0.196
6.702	4.943	1.667	0.301	0.180
6.509	4.745	1.623	0.860	0.529
6.467	4.577	1.606	0.480	0.299
6.226	4.553	1.566	0.662	0.422
5.920	4.020	1.589	0.442	0.278
6.260	4.665	1.728	1.405	0.813
6.892	5.586	1.666	1.245	0.747
7.474	6.913	1.908	1.105	0.579
6.229	4.281	1.642	0.236	0.143
5.607	3.340	1.285	0.100	0.078
5.677	3.561	1.365	0.120	0.087
6.444	4.526	1.485	0.121	0.081
5.621	3.606	1.385	0.100	0.072
5.927	4.078	1.326	0.139	0.105
6.873	5.397	1.708	0.140	0.082
6.885	5.333	1.688	0.121	0.071
7.304	6.144	1.806	0.179	0.099
7.946	7.038	1.664	0.139	0.084
7.089	5.760	1.643	0.140	0.085
7.451	6.694	1.784	0.239	0.134
7.607	6.638	1.649	0.221	0.134

Figure 4.14: Results of examining the braking process without ABS.

4.3.3 Decrease the Braking Distance

The formula for calculating the braking distance d_b depends on the velocity at the beginning of the braking process v_{max} and on the braking deceleration a [29]:

$$d_b = \frac{v_{max}^2}{2a}$$

Therefore, a square root function (due to conversion) is fitted to the data collected in table 4.13 and table 4.14. For the fitting, the outlier with a braking distance of 10[m] is neglected due to the big sensitivity of the fitting to outliers.
The functions resulting from fitting the braking distances are very similar. For instance, the difference in braking distance for $v_{max} = 8\,[\mathrm{m/s}]$ is $0.095\,[\mathrm{m}]$. This is a small difference, especially when the big standard deviation is considered (see table 4.4).

$$d_{b,\,ABS\,on} = 0.114049 \cdot v_{max}^2$$
$$d_{b,\,ABS\,off} = 0.112554 \cdot v_{max}^2$$

The error $\epsilon\,[\mathrm{m}]$ is calculated as the difference between the actual braking distance d_b and the braking distance calculated with the fitted function d_{fit}. For the mean, the standard deviation and the CV, the outlier is neglected as well. The results are displayed in table 4.4.
Figure 4.15 shows both fitted functions and all collected data points for ABS active/passive.

	Error $\epsilon\,[\mathrm{m}]$		
ABS on/off	mean μ	standard deviation σ	CV
on	0.161	0.115	0.714
off	0.137	0.123	0.896

Table 4.4: Error $\epsilon\,[\mathrm{m}]$ between calculated and actual braking distance.

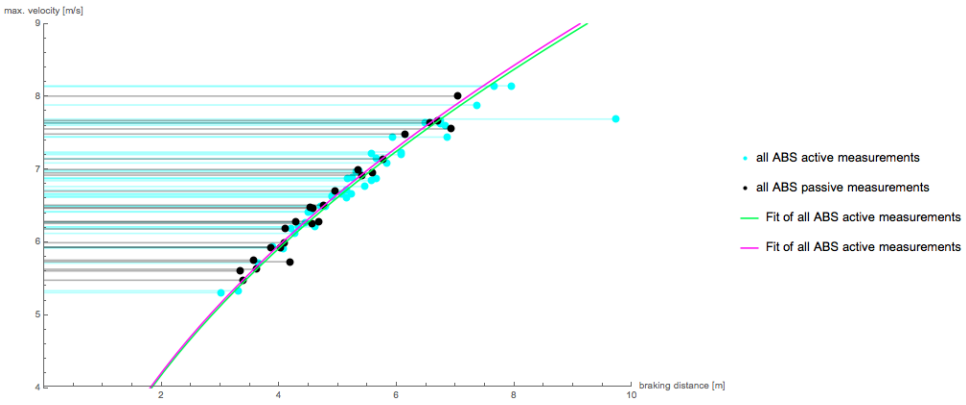

Figure 4.15: The measured braking distances for ABS active/passive.

4.3.4 Discussion

It is not possible with the current implementation to decrease the braking distance. The results for the braking with and without ABS were almost the same. Additionally, the braking distance has a big standard deviation. Even if an ABS would be implemented that in average reduces the braking distance, it is no reliable. An ABS of this kind can not be used to improve features such as the "Emergency Braking Demonstration".

The observed outlier is examined (see fig. 4.16) and compared to "normal" braking process plots. Unfortunately, it is detectable why the braking distance was 2.8[m] longer than expected. It is not unusual that both slip values are high during approximately one second. The velocity plot shows that the velocity started decreasing after 0.5 seconds, but it is not clear what caused this delay in deceleration.

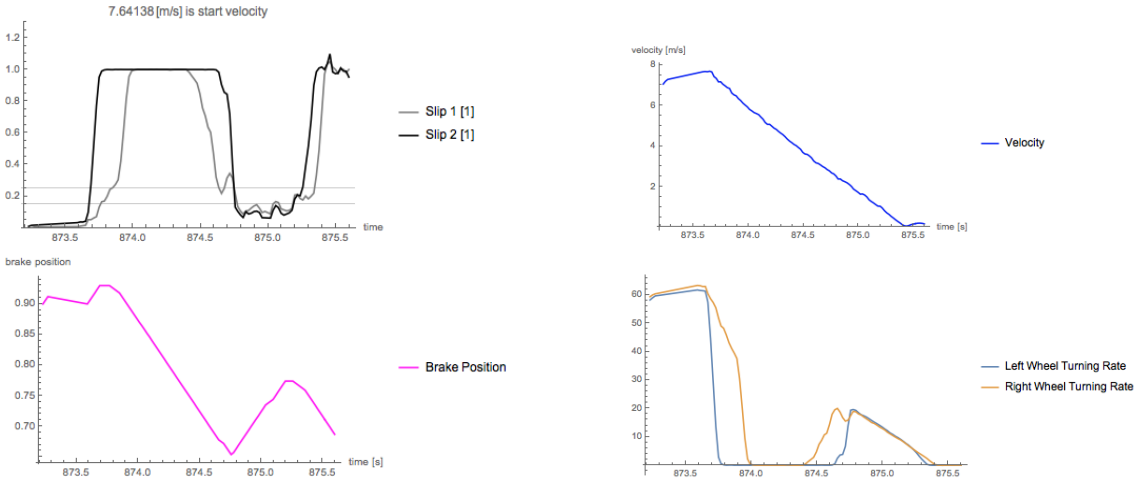

Figure 4.16: Plot of the braking process of the outlier.

With the ABS active, it is possible to nearly double the time during which the slip is under 25%. This provides steerability during the full braking maneuver.

Chapter 5

Conclusion

The goal of this thesis was to implement driver assistance systems on the go-kart that support the progress of the IDSC go-kart project as a whole. In the scope of this thesis, three different ADAS are implemented. For each, the respective objectives are stated in the beginning (refer to chapter 2). Based on these, the features were evaluated.

5.1 Electric Power Steering

The EPS is the most relevant feature out of the three, because it is already used regularly on the go-kart. Steering with power steering is a lot more comfortable for the driver, therefore most students on the go-kart use it while conducting their experiments.
An exception to this is the racing situation. Here, it is mostly a question of personal preference whether the EPS is active or passive. The professional go-kart driver that visited the go-kart project to race against the MPC did not use it.

The evaluation of the EPS shows that the aligning torque is compensated completely (refer to section 4.1.2). As a consequence, the PID used in modules such as the MPC or the Pure Pursuit Module (responsible for curve following) is not counteracted by the aligning torque anymore (refer to section 2.2), when the EPS is active. So, J. Hakenberg already added the EPS within these modules. As a project for future work, the PID controller could be reworked: The I-part was introduced due to the aligning torque, so it could be possible to simplify the PID controller to a PD controller.

5.2 Lane Keeping Assist

The lane keeping assist is more a gadget than an actual feature on the go-kart, since its impact on other projects is small. However, it was particularly interesting to apply the new clothoid planning method, implemented on the go-kart by J. Gächter. Within the scope of the lane keeping assist, it was possible to show how the clothoid planning can be used to gently lead the go-kart back into a desired area/direction.

5.3 Anti-lock Braking System

The implementation of the ABS was a medium success, since it was not possible to reduce the braking distance. However, the advantages of providing more steerability during a full braking are clear. The vision of the IDSC go-kart project is to carry out research on the edge cases and extreme situations of autonomous driving. Modules like the MPC can use the ABS for further examinations of extreme braking maneuvers.

With the approach outlined in section 3.4, the slip values are rarely within the range of 0.15-0.25. If a real improvement of the ABS is sought, one should try to implement a controller which is responsible for keeping the slip within the desirable range. The problem of controlling the slip is that two outputs (left and right slip) have to be controlled with one parameter (braking position). Different control approaches could be compared on this problem.

Bibliography

[1] EU Kommission für Verkehr. Zahl der Verkehrstoten in der EU leicht zurückgegangen - Europas Strassen weltweit am sichersten, April 2018. Available at `https://ec.europa.eu/germany/news/20180410-strassensicherheit_de`, accessed: 2019-08-04.

[2] K. Rumar. The basic driver error: late detection. *Ergonomics*, 33:1281–1290, 1990.

[3] J.R. Treat, N.S. Tumbas, S.T. McDonald, D. Shinar, R.D. Hume, R.E. Mayer, R.L. Stansifer, N.J. Castellan. Institute For Research in Public Safety, Indiana University. *Tri-level study of the causes of traffic accidents: final report.* 1979.

[4] J.R. Treat. *A study of precrash factors involved in traffic accidents.* 1980.

[5] K. Bengler, K. Dietmayer, B. Farber, M. Maurer, C. Stiller, H. Winner. Three decades of driver assistance systems: Review and future perspectives. *IEEE Intelligent Transportation Systems Magazine*, 6:6–22, 4 2014.

[6] EU Commission for Transportation. Vehicle safety systems, 07 2009. Available at `https://ec.europa.eu/transport/themes/its/road/application_areas/vehicle_safety_systems_en`, accessed: 2019-08-04.

[7] S.A. Ferguson. The effectiveness of electronic stability control in reducing real-world crashes: A literature review. *Traffic Injury Prevention*, 8(4):329–338, 2007. PMID: 17994485.

[8] 40 Jahre ABS, September 2018. Available at `https://www.bosch-presse.de/pressportal/de/de/40-jahre-antiblockiersystem-abs-von-bosch-169700.html`, accessed: 2019-08-04.

[9] IDSC autonomous gokart racing short video. Available at `https://www.youtube.com/watch?v=bmIQxtiAzhQ`, accessed: 2019-08-11.

[10] US Departement of Transportation, National Highway Safety Administration. Factors related to fatal single-vehicle run-off-road crashes. Available at `https://crashstats.nhtsa.dot.gov/Api/Public/ViewPublication/811232`, accessed: 2019-08-09.

[11] US Departement of Transportation, National Highway Safety Administration. Run-off-roads crashes. Available at `https://crashstats.nhtsa.dot.gov/Api/Public/ViewPublication/811500`, accessed: 2019-08-09.

[12] American Association of State Highway and Transportation Officials. *Driving Down Lane-Departure Crashes - A National Priority.* 04 2008.

[13] Lane departure warning system. Available at `https://en.wikipedia.org/wiki/Lane_departure_warning_system`, accessed: 2019-08-09.

[14] AGCO Automotive Cooperation. Wheel alignment, camber and caster, 07 2019. Available at `http://www.agcoauto.com/content/news/p2_articleid/176`, accessed: 2019-08-04.

[15] A. Aly, E.-S. Zeidan, A. Hamed, F. A. Salem. An antilock-braking systems (ABS) control: A technical review. *Intelligent Control and Automation*, 02, 01 2011.

[16] Technical reports of the idsc go-kart project. Available at `https://github.com/idsc-frazzoli/retina/blob/master/doc/reports.md`, accessed: 2019-08-12.

[17] V. Govender, S. Müller. Modelling and position control of an electric power steering system. *IFAC-PapersOnLine*, 49:312–318, 01 2016.

[18] C. C. Chung W. Kim, Y. S. Son. Torque-overlay-based robust steering wheel angle control of electrical power steering for a lane-keeping system of automated vehicles. *IEEE Transactions on Vehicular Technology*, 65(6):4379–4392, 06 2016.

[19] M.K. Hassan, N.A.M. Azubira, H.M.I. Nizama, S.F. Toha, S.K.K. Ibrahimad. Optimal design of electric power assisted steering system (EPAS) using GA-PID method. *Procedia Engineering*, 41:614–621, 12 2012.

[20] B.T. Christian, A.S. Rohman, A. Sasongko, L. Bagaspratomo, C. Agustina. The prototype development of electronic control unit for electric power steering. In *Proceedings of the Joint International Conference on Electric Vehicular Technology and Industrial, Mechanical, Electrical and Chemical Engineering (ICEVT IMECE)*, pages 247–252, 11 2015.

[21] H. Zhang, Y. Zhang, J. Liu, J. Ren, Y. Gao. Modeling and characteristic curves of electric electric power steering systems. 15:1390–1393, doi=10.1109/PEDS.2009.5385774, 2011.

[22] M. H. Lee, K. H. Seung, J.Y. Choi, K.S. Yoon. Improvement of the steering feel of an electric power steering system by torque map modification. *Journal of Mechanical Science and Technology*, 19(3):792–801, 03 2005.

[23] H. Chen, Y. Yang, R. Zhang. Study on electric power steering system based on ADAMS. *Procedia Engineering*, 15:474–478, 2011.

[24] D. Lee, K. Kim, S. Kim. Controller design of an electric power steering system. *IEEE Transactions on Control Systems Technology*, 26(2):748–755, 03 2018.

[25] S. Brunner, M. Harrer, M. Höll, D. Lunkeit", editor="Harrer M., Pfeffer P. *Steering Handbook*, pages 426–427. Springer International Publishing, 2017.

[26] A. Marouf, M. Djemai, C. Sentouh, P. Pudlo. A new control strategy of an electric-power-assisted steering system. *Vehicular Technology, IEEE Transactions on*, 61:3574–3589, 10 2012.

[27] R. F. Riesenfeld J. M. Lane. A theoretical development for the computer generation and display of piecewise polynomial surfaces. *IEEE Transactions on Pattern Analysis and Machine Intelligence*, PAMI-2(1):35–46, 01 1980.

[28] Euler spiral (Clothoid). Available at `https://en.wikipedia.org/wiki/Euler_spiral#Formulation`, accessed: 2019-08-04.

[29] Braking distance. Available at `https://en.wikipedia.org/wiki/Braking_distance`, accessed: 2019-08-12.

Appendix A

Experiments

A.1 Electric Power Steering

A.1.1 Reducing the Applied Driver Torque

Description of the Experiment

A specific track is driven twice under similar conditions, once with (red) and once without (blue) EPS. Then, the applied driver torque per meter is measured and compared. The order of the plots corresponds to table 4.1.

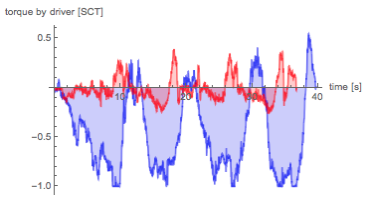

Figure A.1: [circle, slow]

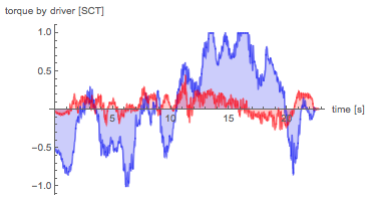

Figure A.2: [circle, medium]

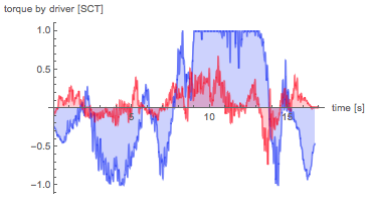

Figure A.3: [circle, fast]

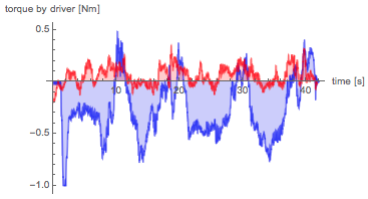

Figure A.4: [circle, slow]

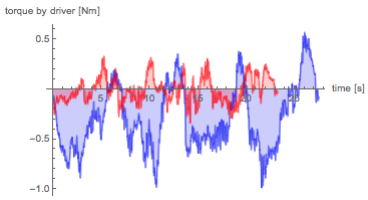

Figure A.5: [circle, medium]

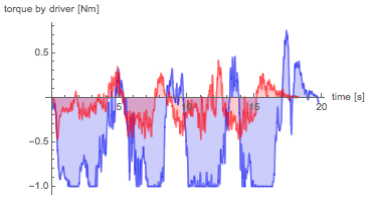

Figure A.6: [circle, fast]

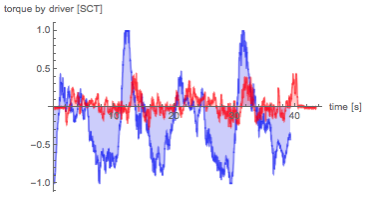

Figure A.7: [eight, slow]

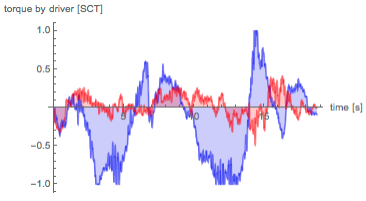

Figure A.8: [eight, medium]

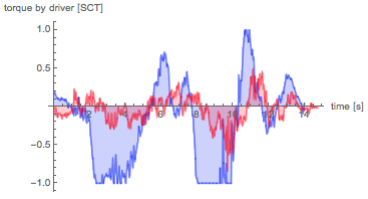

Figure A.9: [eight, fast]

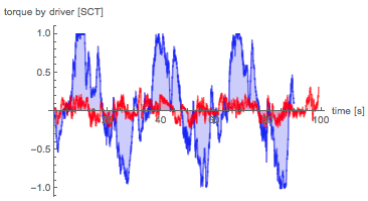

Figure A.10: [eight, slow]

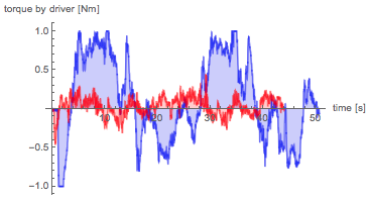

Figure A.11: [eight, medium]

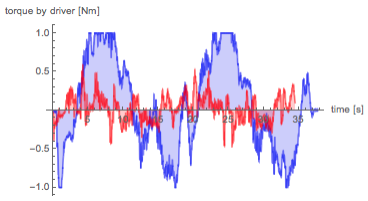

Figure A.12: [eight, fast]

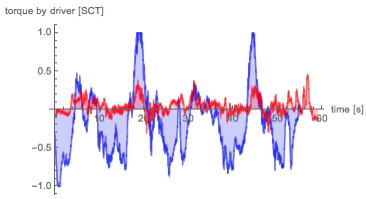

Figure A.13: [track, slow]

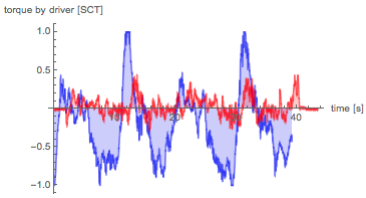

Figure A.14: [track, medium]

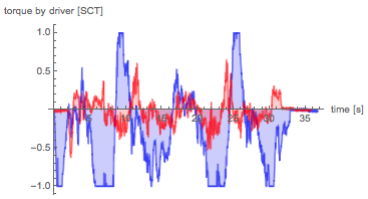

Figure A.15: [track, fast]

A.1.2 Compensation of Aligning Torque - Validation

Description of the Experiment

The steering wheel is deflected from its initial position. Then, the go-kart is accelerated, while no driver torque is applied. This procedure is repeated, with and without EPS.

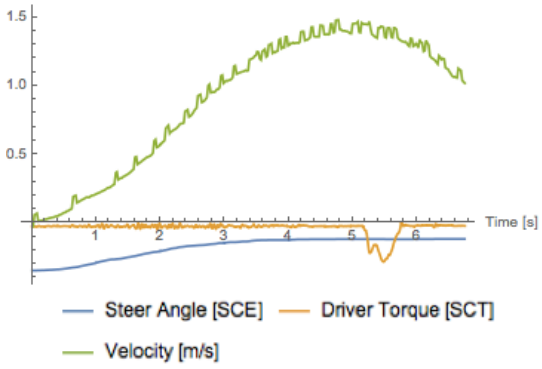

Figure A.16: without EPS

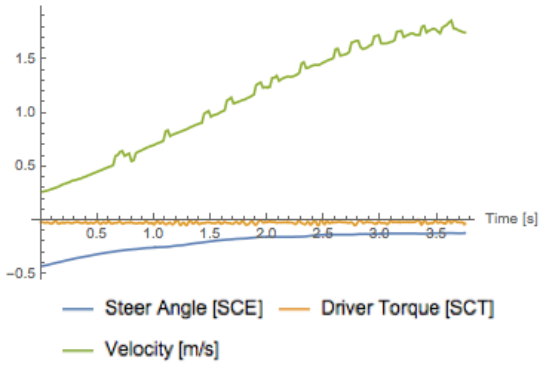

Figure A.17: without EPS

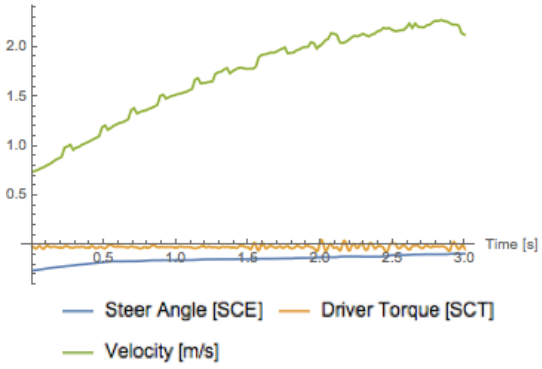

Figure A.18: without EPS

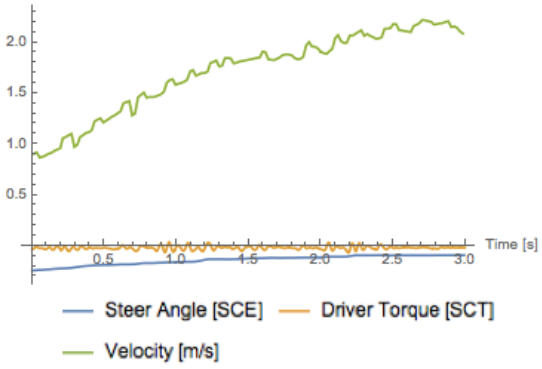

Figure A.19: without EPS

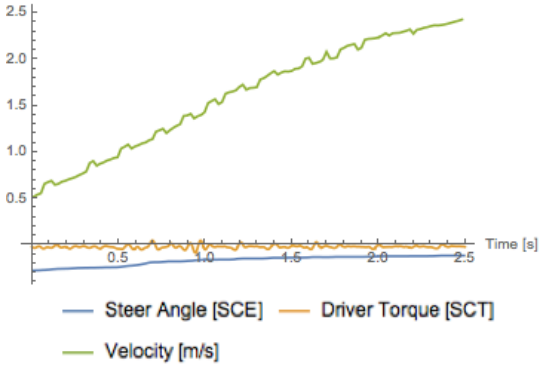

Figure A.20: without EPS

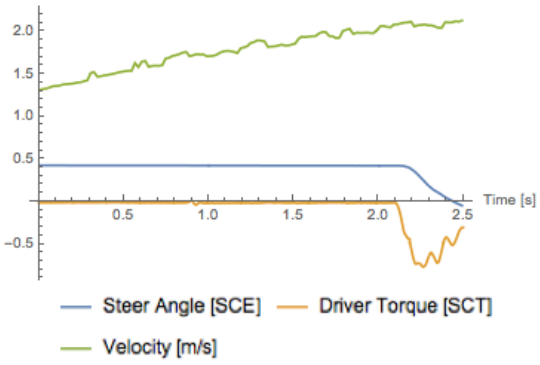

Figure A.21: with EPS

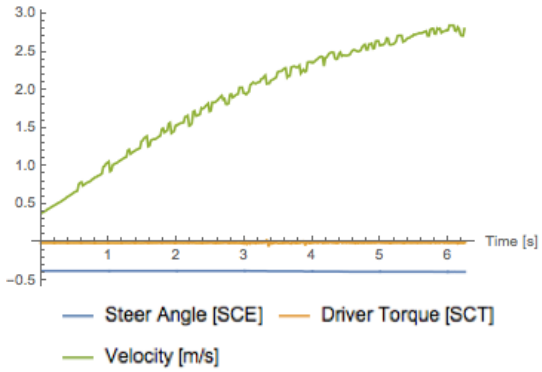

Figure A.22: with EPS

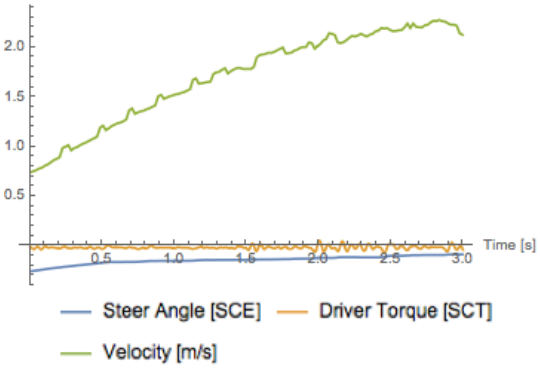

Figure A.23: with EPS

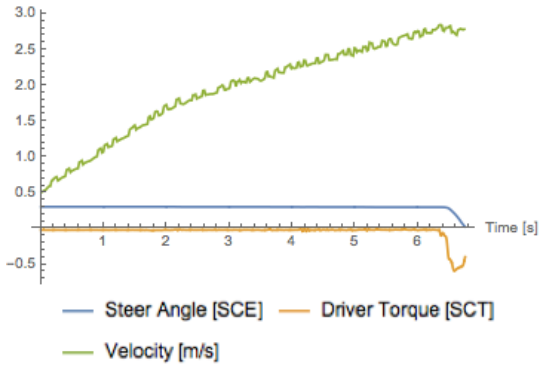

Figure A.24: with EPS

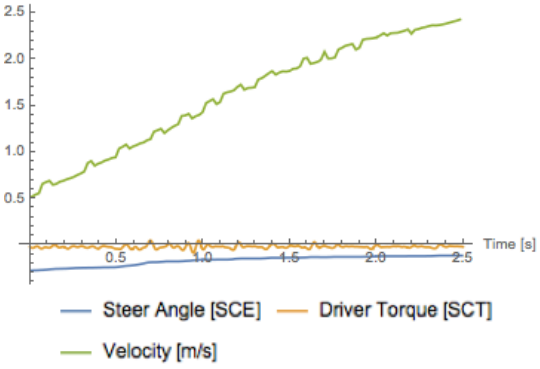

Figure A.25: with EPS

A.2 Anti-lock Braking System

The plots shown below are picked randomly. For each braking process, the slip of both wheels, the decline of the velocity of the vehicle and of the wheels, and the brake position is displayed. Overall, 42 full brakings with ABS active and 25 full brakings with ABS passive are conducted and logged.

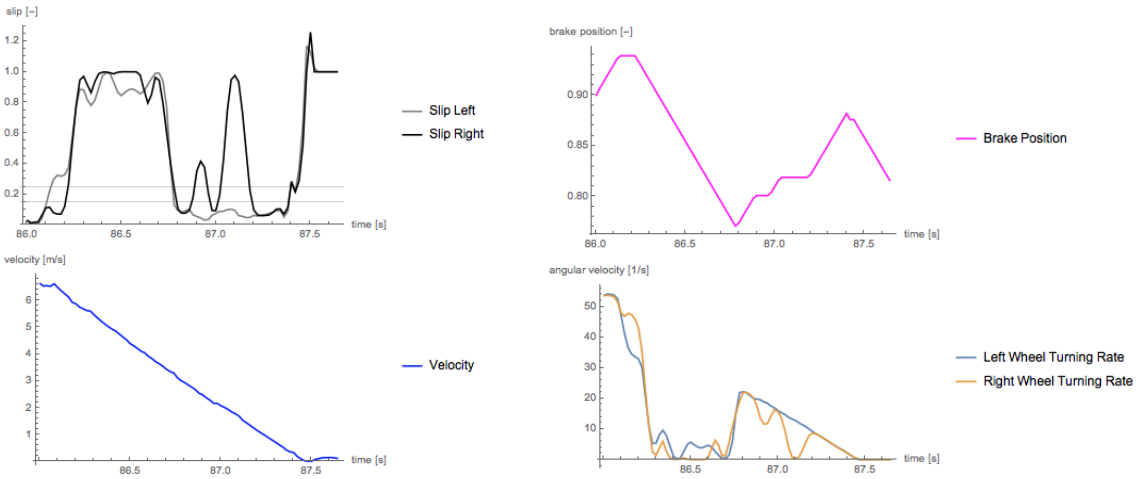

Figure A.26: Example plot of a braking process with ABS active.

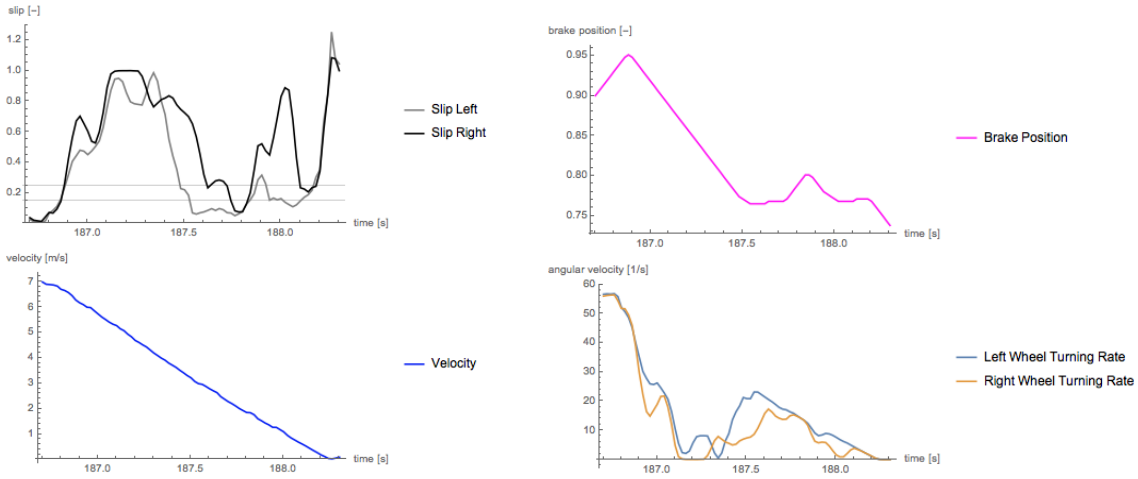

Figure A.27: Example plot of a braking process with ABS active.

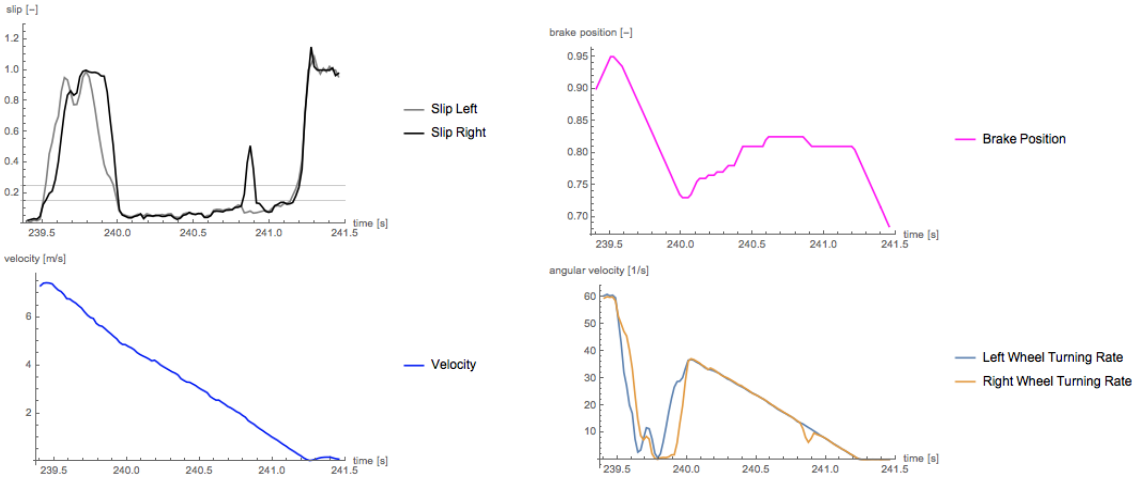

Figure A.28: Example plot of a braking process with ABS active.

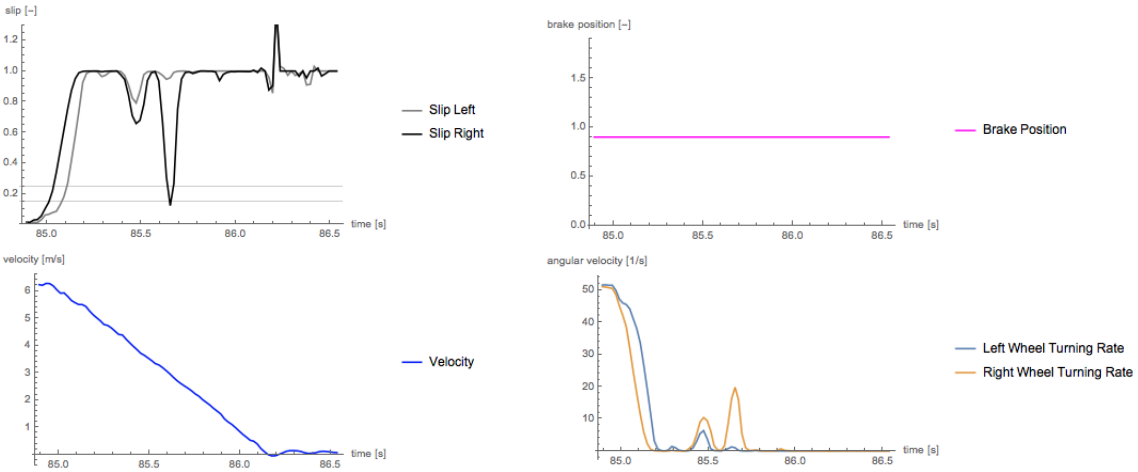

Figure A.29: Example plot of a braking process with ABS passive.

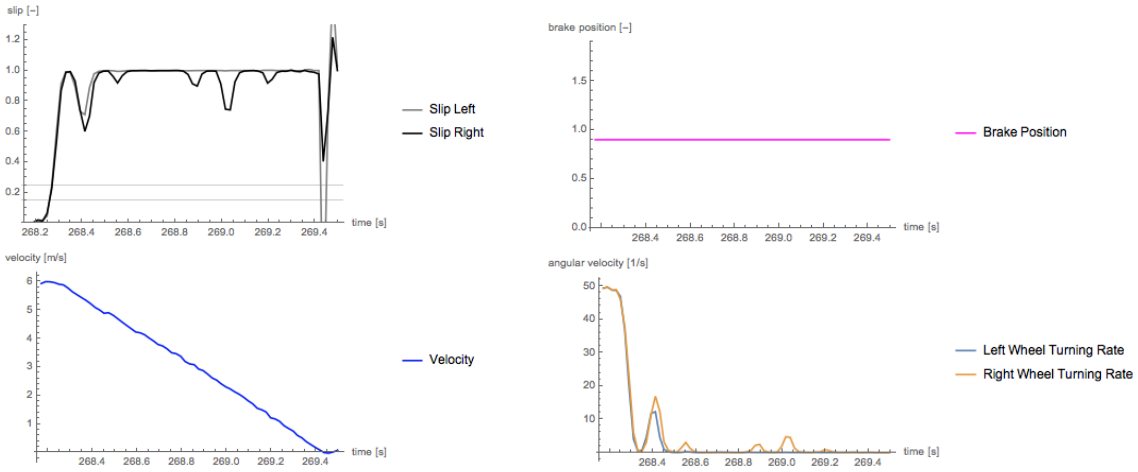

Figure A.30: Example plot of a braking process with ABS passive.

Appendix B

Source Code

The code and development history of the project are hosted on the collaborative coding platform Github and are publicly available at the address https://github.com/idsc-frazzoli/retina.